NASA TN D-1382

2

TECHNICAL NOTE

D-1382

SLIPSTREAM FLOW AROUND SEVERAL TILT-WING VTOL AIRCRAFT MODELS OPERATING NEAR THE GROUND

By William A. Newsom, Jr., and Louis P. Tosti

Langley Research Center
Langley Station, Hampton, Va.

NATIONAL AERONAUTICS AND SPACE ADMINISTRATION

WASHINGTON September 1962

NATIONAL AERONAUTICS AND SPACE ADMINISTRATION

TECHNICAL NOTE D-1382

SLIPSTREAM FLOW AROUND SEVERAL TILT-WING VTOL AIRCRAFT MODELS OPERATING NEAR THE GROUND

By William A. Newsom, Jr., and Louis P. Tosti

SUMMARY

A collection of data from a number of brief investigations made with three different models to determine the character of the slipstream flow along the ground is presented for multiple-propeller tilt-wing VTOL aircraft configurations operating near the ground. In general, the tests involved tuft surveys and slipstream dynamic-pressure measurements for several tilt-wing VTOL models. A more extensive series of tests, including some measurements of the erosion of gravel by the slipstream and some measurements of the unsteady rolling, yawing, and pitching moments, was also made on one of the models operating in the hovering condition near the ground.

The results of the flow studies indicated the presence of a stronger and deeper slipstream flow along the center line of the aircraft, and to some extent along parallel planes between adjacent propellers (on one wing), than to the side of the aircraft. This effect is caused by an intensification of the individual slipstreams as they meet at the planes of flow symmetry. The intensified flow along the center line of the aircraft is amplified by the presence of the fuselage and causes the dynamic pressure to be greater in front of the aircraft than would be expected on the basis of the slipstream of the individual propellers. In the erosion tests it was found that gravel, if sufficiently small, was rapidly eroded by the slipstream and that this gravel could be thrown high into the air if it struck even very small fixed obstacles on the ground (obstacles with a height less than the diameter of the gravel). Results of the investigation of moment fluctuations indicated that there are large, erratic variations of rolling, yawing, and pitching moments and that the propellers, reacting to an erratic inflow from the recirculating slipstream, are the primary source of these moments.

INTRODUCTION

An understanding of the flow field around the aircraft is necessary for understanding such problems as ground erosion, recirculation of dust

and debris, ground effect on lift and moments, and other related difficulties experienced by multipropeller VTOL aircraft operating near the ground. The present paper has been prepared to present some data on this subject collected over a period of time with several different small-scale tilt-wing VTOL aircraft models. The configurations tested included two 2-propeller models and one 4-propeller model. The tests consisted primarily of measurements of the direction and dynamic pressure of the slipstream flow along or near the ground when the models were operated in the hovering condition very close to the ground. In addition, a brief investigation was made of the erosion and possible recirculation of gravel caused by the slipstream. An investigation was also made of the fluctuations of the aerodynamic forces and moments of one of the models as part of a study of the unsteady or rough behavior of VTOL aircraft when hovering near the ground.

SYMBOLS

D	propeller diameter, ft
q	local dynamic pressure, lb/sq ft
q_N	average dynamic pressure from slipstream of propeller, $\frac{\text{Thrust}}{\pi D^2/4}$, lb/sq ft
q_s	dynamic pressure measured parallel to the surface of the ground, lb/sq ft
h	height of propeller plane above ground, ft
x	fore and aft distance of survey station from wing hinge line, ft
y	spanwise distance of survey station from plane of symmetry, ft
y'	spanwise distance of survey station from plane midway between two propellers on the same side of fuselage, ft
z	height of survey station above ground, ft
M_X	rolling moment, ft-lb
M_Y	pitching moment, ft-lb
M_Z	yawing moment, ft-lb

Subscript:

max maximum

MODELS

Three different model configurations were used in the tests. These configurations, which are shown in figure 1, are as follows:

(1) One model was a small-scale general research model having four 3-blade propellers (fig. 1(a)). The model was designed to resemble a transport-type configuration and had a high-aspect-ratio wing pivoted at the 65-percent-chord station.

(2) Another model was a 1/8-scale model of the Hiller X-18 VTOL test bed (fig. 1(b)). The model had two 6-blade dual-rotating propellers mounted on a low-aspect-ratio wing that was pivoted at the 34.8-percent-chord station. Additional information on this model is presented in reference 1.

(3) The third model was a 1/4-scale model of the VZ-2 (Vertol 76) VTOL test bed (fig. 1(c)). The model had two 3-blade propellers mounted on a straight wing which was pivoted at the 37-percent-chord station. Additional information on this model is presented in reference 2.

TESTS

Flow Along the Ground

The investigations were concerned primarily with the character of the slipstream flow along the ground caused by tilt-wing VTOL aircraft during take-off and landing. For these tests the models were mounted on a boom located in a large open indoor test area. Figure 2 shows a photograph of an installation very similar to the setup used in these tests. The end of the boom could be lowered or raised so that the models could be positioned at heights which corresponded to lift-off. The wing incidence angles were set to correspond to a hovering condition (zero fore and aft force). The disk loading for various tests was from 5 to 7 pounds per square foot and represented approximately the dynamically scaled hovering disk loading of the various airplanes.

The slipstream flow along the ground was measured by using a survey rake of very small tubes placed parallel to the ground at various stations around the model. Figure 3 shows, for each of the three models,

the positions at which the survey rake was placed to determine the strength of the flow field about the models. The small circular symbols on these planform plots indicate the rake locations. At each of these locations the tubes of the rake were in the vertical planes indicated in the figure to give a vertical profile of the slipstream at each location.

Additional Tests With VZ-2 Model

In addition to the surveys of flow velocity parallel to the ground, which were made on all three models, the three following series of tests were made with the 1/4-scale model of the VZ-2:

Upward-flow study.- A survey of the flow directly beneath the VZ-2 model was made to determine the dynamic pressure of the upward flow near the plane of symmetry which had been shown to exist under tilt-wing VTOL aircraft by the tuft tests of reference 3. A survey was made of the flow in a spanwise plane through the wing pivot and down the center line of the fuselage as well as around the sides of the fuselage. For this test a single tube was used. The single tube was adjusted to aline with local flow by using a wool tuft. In this manner, not only the magnitude of the dynamic pressure but, by observation, the approximate direction of the flow could be determined.

Erosion study.- For a brief erosion study, the model was set at the take-off height as in the other tests, and a bed of gravel was spread in an approximately circular area extending a few inches outboard of the wing tips and the fuselage extremities on the smooth concrete floor under the model. A square enclosure, 20 feet on a side and 6 inches high, was placed on the floor around the test area to keep the gravel from spreading too far. Two sizes of gravel were used. The larger size would pass through a 0.5-inch mesh screen but not through a 0.25-inch mesh screen. The smaller size would pass through a 0.125-inch mesh screen but not through a 0.0625-inch mesh screen. After the gravel was in place, the model power was brought up rapidly to the scaled-down hovering disk loading of the VZ-2 aircraft (6.33 pounds per square foot), and the effect of the slipstream on the gravel was observed and photographed. Some tests were also made with barriers of various heights fastened to the ground around the layer of gravel to observe their effect in causing particles to be thrown into the air.

Buffet study.- The study of the buffeting experienced near the ground was made with the model mounted on the boom as in the other tests. For this test, however, the output from a strain-gage balance in the model was fed into an oscillograph so that a continuous record of the random rolling, yawing, and pitching moments caused by the slipstream recirculation could be obtained. In order to suppress the input due to propeller

vibration so that the fluctuation of the aerodynamic moments would not be masked, appropriate filters were inserted in the line between the balance and the oscillograph to attenuate frequencies above about 25 cycles per second. Oscillograph records were obtained for the model with tail-fan controls on at $h/D = 3.0$ and $h/D = 1.0$. At $h/D = 1.0$, in addition to the tests of the model configuration with tail-fan controls on, data were also obtained with tail fans off, with the fuselage bottom uncovered and covered, and with the wing alone. In addition to tests with a simple covering on the fuselage bottom, tests were also made with the bottom covered and with 3-inch-wide deflectors drooped 45° and fastened along the lower longerons of the fuselage. In the tests with the wing alone, weights mounted on a boom attached in place of the fuselage were used to reproduce the moment of inertia of the missing fuselage.

RESULTS AND DISCUSSION

General Discussion

One topic which has recently been receiving considerable attention relative to the danger of the high-velocity slipstream flow along the ground from a VTOL aircraft is the blowing over of objects around the take-off and landing area. It has been found that the problem of objects being blown over may be actually less severe for higher-disk-loading VTOL aircraft than for helicopters. Research reported in reference 4 for two aircraft having the same gross weight but different disk loadings indicated that although the high-disk-loading aircraft produces higher dynamic pressures along the ground at distances up to about one rotor diameter (of the larger rotor) from the center line, beyond this point the dynamic pressure is slightly less for the high-disk-loading aircraft than for the low-disk-loading one. Since the slipstream flow along the ground is much thicker for the low-disk-loading rotor, it would appear that at these greater distances where the dynamic pressures are almost equal, the tendency to overturn objects on the ground would be greater for the low-disk-loading rotor.

The example of the relative strength of the flow field of high- and low-disk-loading rotors presented in reference 4 is for the case of a single-rotor machine. The data of reference 4 also show that the flow field along the ground is different for single-rotor aircraft than for multiple-rotor aircraft. This point is also discussed in reference 3 which presents the results of the tuft tests to show the direction of flow near the ground for a 4-propeller tilt-wing model. The basic flow field caused by the propeller slipstream of a tilt-wing VTOL aircraft at take-off is discussed in reference 3. The results presented show

that the plane of symmetry seems to act as a solid wall through which no flow can pass because of the mirror-image flow on the other side. When the slipstream of the propellers approaches the ground, it tends to spread out in all directions. Since the slipstream cannot flow through the plane of symmetry, the flow at the plane of symmetry must go either upward, forward, or rearward to escape.

Outward Flow Along the Ground

Figures 4, 5, and 6 present the profiles of the dynamic-pressure ratio for the 4-propeller, the Hiller X-18, and the VZ-2 models, respectively. These dynamic-pressure profiles, which were obtained with the survey rake positioned at the stations and in the planes indicated in figure 3, may not always show the maximum dynamic pressure, inasmuch as it seemed certain that the rake was greatly misalined with respect to the ground flow at stations very near the wing-fuselage juncture. These data are summarized in figure 7 in the form of dynamic-pressure contours along the ground. Actually, they are contours of the dynamic pressure at the height above the ground at which the dynamic pressure q was maximum. The solid lines are the contours representing values of dynamic pressure of 0.2, 0.4, 0.6, and 0.8 of the average slipstream q below the propellers, and the dashed lines represent the estimated contour at $q_{s,max}/q_N = 0.4$ based on the single-rotor data of reference 5 for each of the single propellers on the assumption that neither wing nor other propellers were present. The data show that there is a definite buildup in q along the longitudinal center line of the aircraft as compared with the estimated contours for the individual propellers. Note that the 0.4 contour line for the three models, and especially for the Hiller X-18 model (fig. 7(b)), extends farther forward than to the side of the aircraft. Also the contour lines generally extend farther forward than rearward for the three models tested. The distortions of the contour lines for multiple propellers are caused by a combination of effects which include an intensifying effect of the slipstreams coming together at the plane of symmetry, the presence of the fuselage near the ground to concentrate the slipstream flow, the relative directions of propeller rotation, and the influence of the wing in the vertical slipstream immediately below the propellers. At the present state of the art, lack of basic data on the interrelationships of these effects makes it difficult, if not impossible, to explain the exact mechanism causing distortion of the contours and to predict the effects for a new and different configuration.

The curves of figure 8 show the comparative measurements of the dynamic pressure of the outward-flowing sheet of air in the plane of symmetry and in the plane of the wing for the VZ-2 model as indicated by the sketch in the figure. These data are the results of a survey

additional to that of figures 3 and 6 and include data at points farther out from the model and at greater heights above the ground. The data of figure 8 are summarized in figure 9, which shows a plot of the maximum dynamic-pressure ratio at each station as a function of distance outward from the center of the model. These data show that for the smaller distances, the dynamic pressure is greater beside the model than ahead of it and that for greater distances it is greater ahead of the model than beside it. This same result has been found in tests on a full-scale dual-propeller VTOL aircraft as shown in reference 4 and in unpublished results of tests on the full-scale VZ-2 and the Doak VZ-4 aircraft.

The plots of figure 8 show the thick depth of flow in the forward direction in the plane of symmetry as compared with the much thinner depth of flow in the plane of the wing. For example, at the lateral station $y/D = 2.78$ no dynamic pressure could be measured above a height $z/D = 0.18$ but even at the forward station $x/D = 3.43$ a dynamic-pressure ratio q_s/q_N of 0.07 was measured at a vertical height equal to the height of the plane of the propeller disk. This greater depth in the forward direction, and hence greater mass of flow at a given dynamic pressure, probably accounts for the fact that the slipstream persists to greater distances ahead of than beside the model. The thicker slipstream has more air in proportion to its surface area so that it loses less energy due to friction and entrainment of the static air above the slipstream. It was observed and checked with a tuft wand that this flow forward in the plane of symmetry was inclined upward from the horizontal; thus, the flow was expanding in height with increasing distance from the model. This expanding flow is indicated in figure 8 by the crossover of the two curves at a height above one propeller diameter. The persistence of the flow along the plane of symmetry for the VZ-2 model at greater heights above the ground and at an appreciable distance from the model can also be seen from figure 10. A cross section has been taken at approximately station III for planes 0, 2, 3, and 4 (see sketch in fig. 10) and contours of q_s/q_N have been plotted. The data show, in a better perspective than the basic data figures, the very high but narrow jet of air squirting out forward along the plane of symmetry.

It has been observed by others in tests of a twin-propeller VTOL aircraft when operated over dry snow as reported in reference 6 that a large cloud of snow obscured the pilot's visibility ahead of the aircraft but that it was possible for the pilot to remain oriented since visibility was retained just to the right and left of "dead ahead." This obscured visibility was apprently caused by the light snow particles being borne up by the deep flow along the plane of symmetry as described in the previous paragraph.

Figure 11 shows that the intensifying effects of multiple slipstreams is not limited to the major plane of symmetry of the airplane.

The figure shows dynamic-pressure profiles taken near the ground at various stations in the plane of the wing and forward in a plane between the two propellers on the same side of the fuselage as indicated by the small sketch in the figure. These data are summarized in figure 12 which shows a plot of the maximum dynamic pressure at each station as a function of the distance outward from a point directly between the propellers. The data show that, just as was the case along the fuselage center line, between two propellers, the dynamic pressure is higher along a plane normal to the wing between two adjacent propellers on the same side of the wing for the greater distances from the reference point between the propellers.

Upward Flow of Recirculating Slipstreams

While performing a taxiing turn with the wing tilted up 76° after landing on a macadam overrun covered with loose and embedded gravel, the VZ-2 aircraft was damaged when gravel was thrown up by the slipstream. This accident is described in detail in reference 7. All blades of both the propellers and tail fans sustained some damage, as did the first-stage stator and rotor blading of the engine. The aircraft structure itself was not damaged but the upwash deposited a great deal of dirt and small stones in the cockpit and open fuselage. The direction of upward flows which could conceivably have caused the gravel to have been lifted into the propellers and engine is shown in reference 3, but no indication of the dynamic pressure was obtained. An extensive survey of the flow field around the 1/4-scale VZ-2 model in the hovering condition was therefore made, and the results are shown in figures 13 and 14. Since the pressure probe was alined with the local flow it is possible to present, along with the plot of dynamic-pressure ratio, an indication of the approximate angle of flow at each survey point. The erratic appearance of some of the curves, particularly for the pressure measurement made along the center line of the fuselage (fig. 13(a)), is believed to be the result of random fluctuations in the flow due to the turbulence and to the instability of the flow under the fuselage.

The effect of the fuselage on the upward flow in the plane of symmetry can be seen in figure 13(a). The fuselage was originally uncovered on the bottom and the top, as is the full-scale VZ-2, so that the flow tended to continue up through the fuselage. However, when the bottom of the fuselage was covered, instead of a gradual change of flow angle from vertical to horizontal as the probe was moved forward or rearward from the area of the wing-fuselage intersection, the upward flow was forced by the fuselage to a horizontal direction almost immediately. The effect of the covered fuselage in preventing the slipstream along the aircraft center line from diffusing upward tended to amplify the slipstream intensifying effect and to give higher velocities and a more horizontal-flow direction in the plane of symmetry.

Figure 14 shows the strength and approximate direction of the slipstream measured in a spanwise plane passing through the wing pivot. The curves show the very rapid decrease in dynamic pressure outboard of the propeller disk indicating the small depth of the outward flowing sheet of air. The low dynamic pressure under the center of the propeller disk is evidently caused by the large hub and nacelle and the lower thrust of the root sections of the propeller. It can be seen also that even though covering the bottom of the fuselage had no effect on the direction of flow, the magnitude of the dynamic pressure in the inboard portion of the plane was increased.

Analysis of the dynamic pressures of the upward flows around the model showed that the dynamic pressures were far too low to have lifted gravel of the size which caused the damage to the VZ-2 aircraft reported in reference 7. Ground erosion tests with scale-size gravel were therefore run to investigate this problem further.

Ground Erosion Tests

The first test to determine the erosion due to the slipstream of the model was made by using the larger size gravel which represented gravel about 1 to 2 inches in diameter in a layer thickness of about $2\frac{1}{2}$ inches for the full-scale aircraft. It should be pointed out that gravel which is scaled dimensionally is also dynamically scaled since it is made of essentially the same material, and such factors as the weights and moments of inertia consequently vary according to the dynamic scale relations. It was observed that this gravel was virtually unaffected by the slipstream even though the model propellers were giving scaled hovering thrust. A few fragments slowly moved away from the edge of the gravel layer and slowly slid across the floor, but no real erosion occurred. When the gravel was spread out to a one-rock thickness on one side of the fuselage center line, the slipstream, once it cleared a small hole in the thin layer, would slowly elongate a radial slot in the gravel. It appeared that the slow erosion continued radially from a random starting point somewhere along the contour of the highest dynamic pressure along the ground.

The smaller size gravel which represented gravel about 1/4 to 1/2 inch in diameter and a layer thickness of about $1\frac{1}{2}$ inches for the full-scale aircraft, on the other hand, was rapidly eroded by the slipstream. The photograph of figure 15 shows the pattern of small gravel remaining after about 15 seconds of erosion by the slipstream. The photograph was made with the camera in front of the model; the strips of tape on the floor indicate the outer limits of the nose, the tail, and the

wing tips. It was observed that immediately under the propeller disk the gravel did not blow away as fast as in the area immediately ahead of and behind the plane of the wing. However, it is believed that this could have been influenced by the thickness of the layer of gravel. It was noted that in the plane of symmetry, the gravel along the forward section eroded faster than the gravel on the rear section possibly because of the concentrating effect of the fuselage bottom which on the forward portion was covered and close to the ground and on the rearward portion was uncovered.

It was observed that the gravel was propelled much higher in the air along the plane of symmetry than to the sides, so that a substantial amount of gravel was thrown completely over both the forward and rearward edges of the enclosure. It was also observed that a large portion of the gravel thrown forward and rearward along the plane of symmetry originated from the gravel thrown inward radially from the two propellers. It did not seem that for hovering conditions, such as those represented by the tests, there would have been any gravel thrown up in such a way as to account for the damage reported in reference 7.

A short series of tests was made to observe the effect of a barrier on the gravel flowing outward from the model. Fences from 0.03 to 0.75 inch high were placed on the floor in a semicircle at about $1\frac{1}{4}$ propeller diameters from the propeller center. Gravel which represented a full-scale size of from 1/4 to 1/2 inch for the full-scale VZ-2 aircraft was rapidly eroded by the slipstream and could be thrown up higher than the propeller disk if the gravel struck fixed obstacles on the ground even though the obstacles were smaller than the gravel diameter. All of the barriers caused particles of gravel to bounce high into the air. It seemed that for the barriers tested, the quantity of gravel thrown in the air was roughly proportional to the height of the barrier. The height to which the gravel bounced, however, seemed independent of the height of the barrier. It was believed that if the barriers had been closer to the model, some of the gravel might have been thrown up into the propellers. It also seemed that if the model had been taxiing it could have run into some of the gravel which was thrown upward and forward.

Buffet Tests

The VZ-2 aircraft, as reported in references 8 and 9, experienced buffeting, unsteadiness, and abrupt yaw disturbances while hovering in ground effect. Some results of the model tests to investigate the reasons for these undesirable conditions of the VZ-2 aircraft near the ground are shown in figures 16 and 17. The data of figure 16 are reproductions of the oscillograph records of the yawing, rolling, and pitching

moments measured during some of the tests. The oscillations of about 4 cycles per second shown in these records do not represent an aerodynamic buffeting but are simply the result of vibration of the model at the natural frequency of the support system. In order to summarize the results more clearly, the envelopes of the yawing-moment traces for the various test conditions are presented in figure 17. A comparison of the two top records of figure 17 shows an increase in unsteadiness and random yawing moments when the model was operated near the ground instead of effectively out of ground effect. Removing the tail fans (which had been considered a potential source of erratic yawing moments since they were located in the recirculating slipstream flow) did not appreciably alter the character of the yawing-moment record. A slight improvement was obtained when the bottom of the open-framework fuselage of the model was covered. A further improvement was noted when "deflector flaps" were installed along the bottom corners of the fuselage as shown by the sketch in figure 17, but even in this configuration the buffeting and random moments were considerably worse in ground effect than they were for the basic configuration out of ground effect. The beneficial effect of these latter changes is attributed to a partial blocking of the recirculated flow and directing it away from the propellers. The propellers reacting to an erratic inflow from the recirculating slipstream are apparently the primary source of erratic moments experienced by a tilt-wing VTOL aircraft in the presence of the ground.

The bottom record of figure 17 which was obtained with the wing and propellers alone, appears to be generally similar to that obtained with the 45° deflector flaps. This result may appear surprising at first glance in view of the fact that with the wing and propellers alone there is no fuselage to block the recirculating slipstream to the propellers. One possible compensating factor which may be involved in this case is that without the fuselage, the upward recirculation flow in the plane of symmetry may be smoother and does not extend as far out from the plane of symmetry. Thus, the inflow to the propellers may not be as unsteady as in the case with the fuselage present.

CONCLUSIONS

The following conclusions are drawn from the results of an investigation of the slipstream flow along the ground with several tilt-wing VTOL aircraft models.

1. The results of the flow studies indicated the presence of a stronger and deeper slipstream flow along the center line of the aircraft, and to some extent along parallel planes between adjacent propellers (on one wing), than to the side of the aircraft. This effect is caused by an intensification of the individual slipstreams as they meet at the

planes of flow symmetry. The intensified flow along the center line of the aircraft is further amplified by the presence of the fuselage and causes the dynamic pressure to be greater in front of the aircraft than would be expected on the basis of the slipstream of the individual propellers.

2. Gravel, if sufficiently small, was rapidly eroded by the slipstream and could be thrown high into the air if it struck even very small fixed obstacles on the ground (obstacles with a height less than the diameter of the gravel).

3. In ground effect, the propellers reacting to an erratic inflow from the recirculating slipstream are apparently a primary source of erratic moments experienced by the tilt-wing VTOL aircraft operating near the ground.

Langley Research Center,
National Aeronautics and Space Administration,
Langley Station, Hampton, Va., May 28, 1962.

REFERENCES

1. Tosti, Louis P.: Force-Test Investigation of the Stability and Control Characteristics of a 1/8-Scale Model of a Tilt-Wing Vertical-Take-Off-and-Landing Airplane. NASA TN D-44, 1960.

2. Newsom, William A., Jr., and Tosti, Louis P.: Force-Test Investigation of the Stability and Control Characteristics of a 1/4-Scale Model of a Tilt-Wing Vertical-Take-Off-and-Landing Aircraft. NASA MEMO 11-3-58L, 1959.

3. Newsom, William A., Jr.: Effect of Ground Proximity on the Aerodynamic Characteristics of a Four-Engine Vertical-Take-Off-and-Landing Transport-Airplane Model With Tilting Wing and Propellers. NACA TN 4124, 1957.

4. O'Bryan, Thomas C.: An Investigation of the Effect of Downwash From a VTOL Aircraft and a Helicopter in the Ground Environment. NASA TN D-977, 1961.

5. Kuhn, Richard E.: An Investigation to Determine Conditions Under Which Downwash From VTOL Aircraft Will Start Surface Erosion From Various Types of Terrain. NASA TN D-56, 1959.

6. O'Bryan, Thomas C.: An Experimental Study of the Effect of Downwash From a Twin-Propeller VTOL Aircraft on Several Types of Ground Surfaces. NASA TN D-1239, 1962.

7. Pegg, Robert J.: Damage Incurred on a Tilt-Wing Multipropeller VTOL/STOL Aircraft Operating Over a Level, Gravel-Covered Surface. NASA TN D-535, 1960.

8. Reeder, John P.: Handling Qualities Experience With Several VTOL Research Aircraft. NASA TN D-735, 1961.

9. Ward, John F.: Structural-Loads Surveys on Two Tilt-Wing VTOL Configurations. NASA TN D-729, 1961.

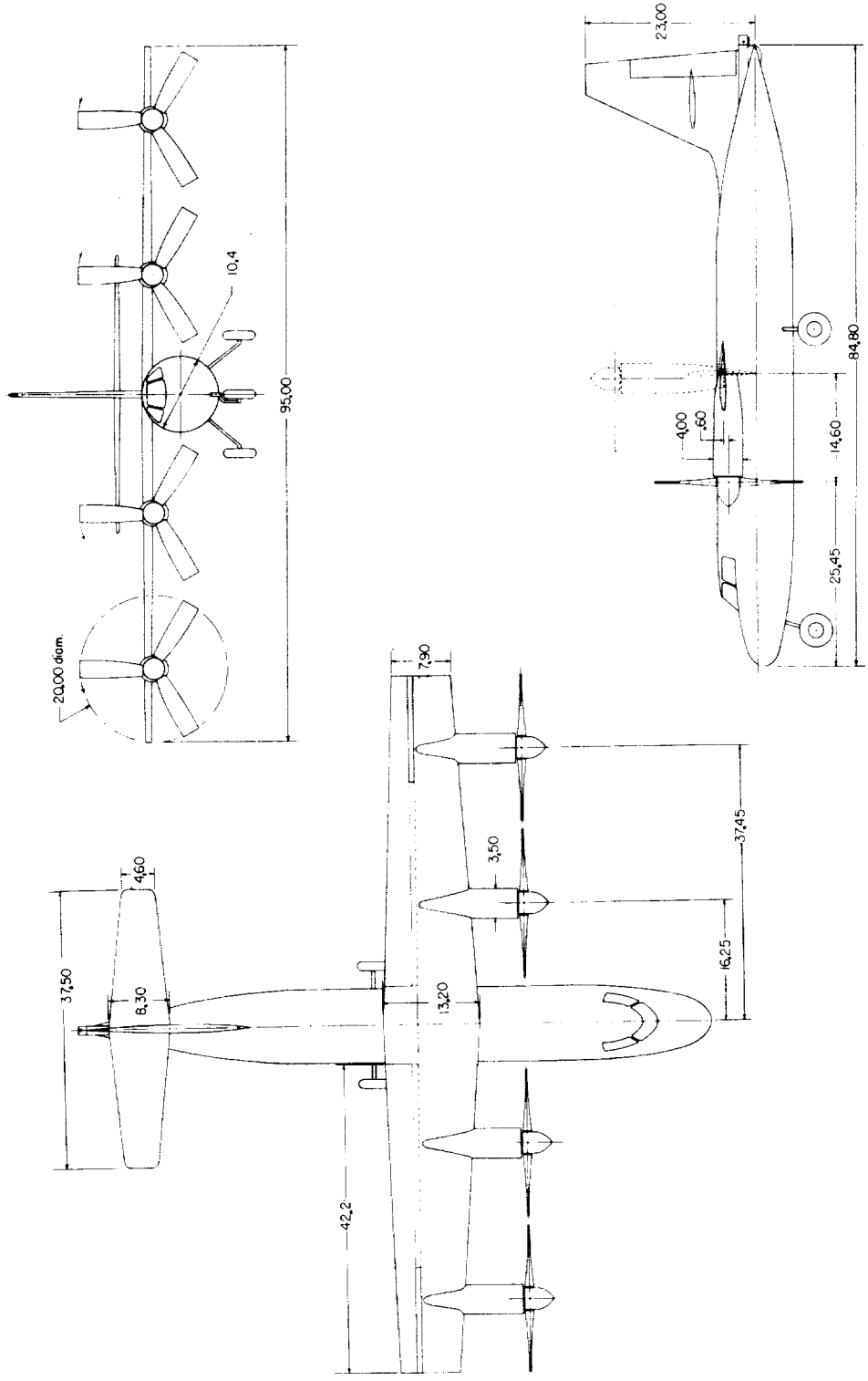

(a) Four-propeller model.

Figure 1.- Three-view drawings of the models used in the investigation. All dimensions are in inches.

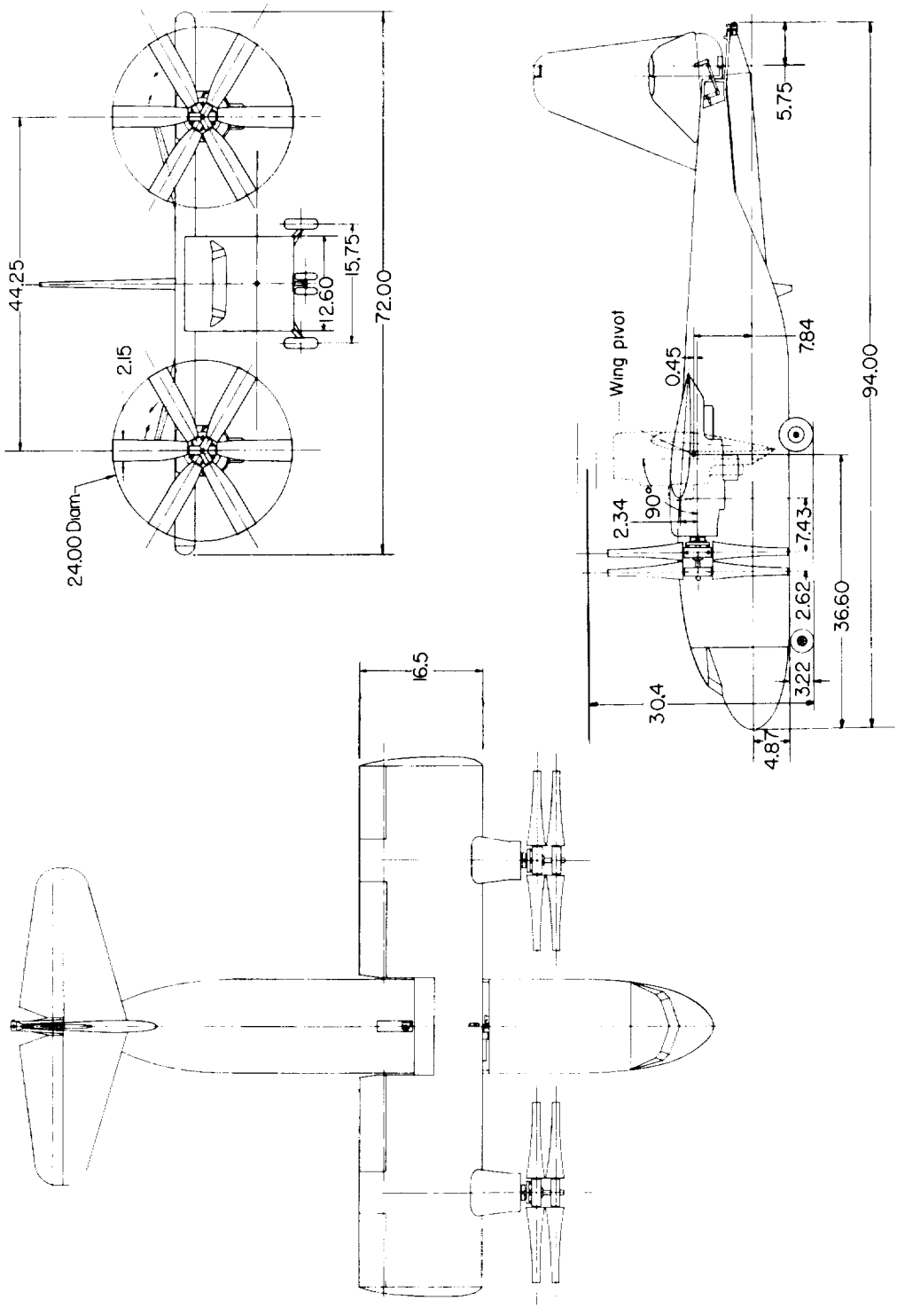

(b) 1/8-scale model of the Hiller X-18.

Figure 1.- Continued.

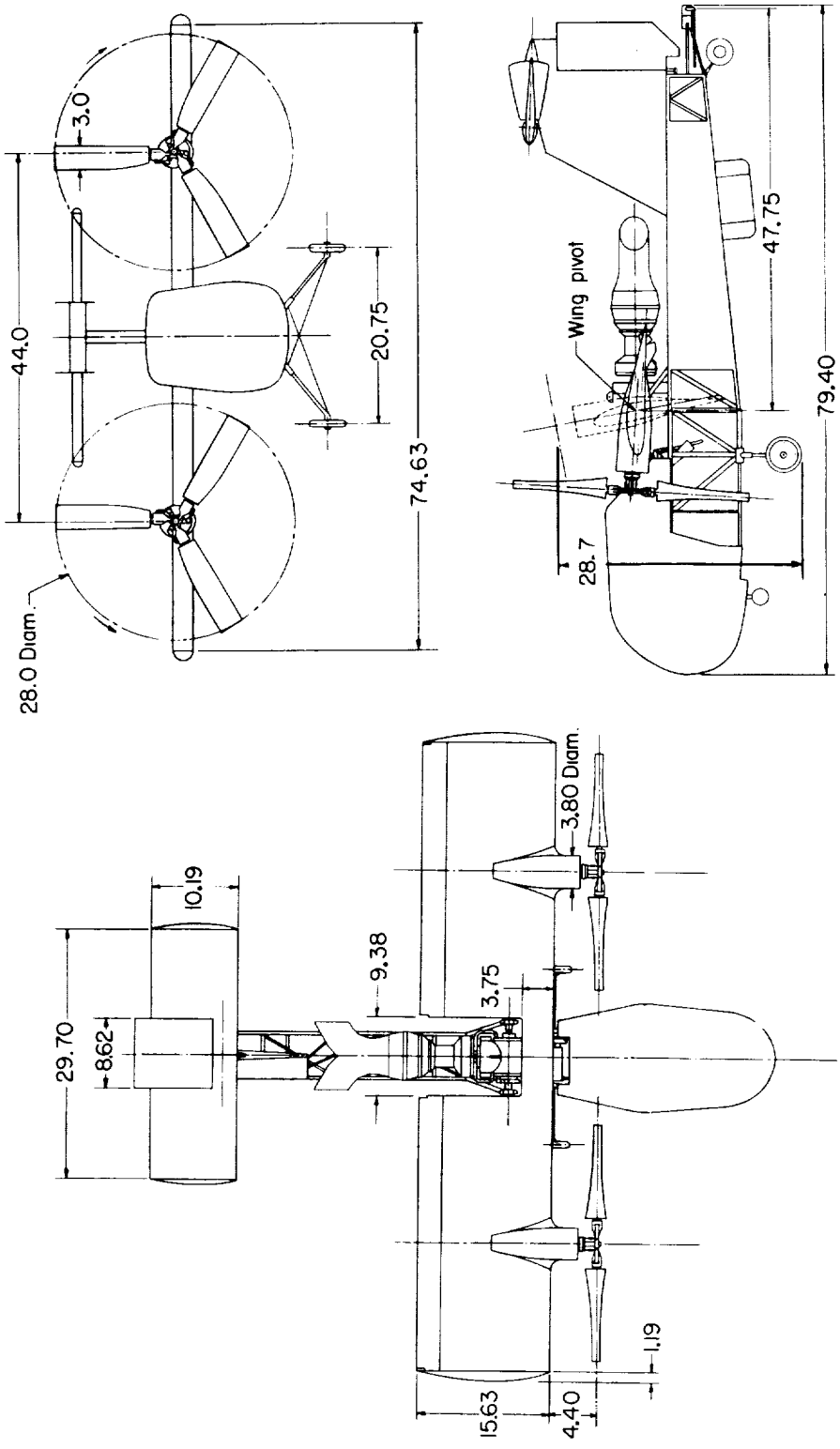

(c) 1/4-scale model of the VZ-2.

Figure 1.- Concluded.

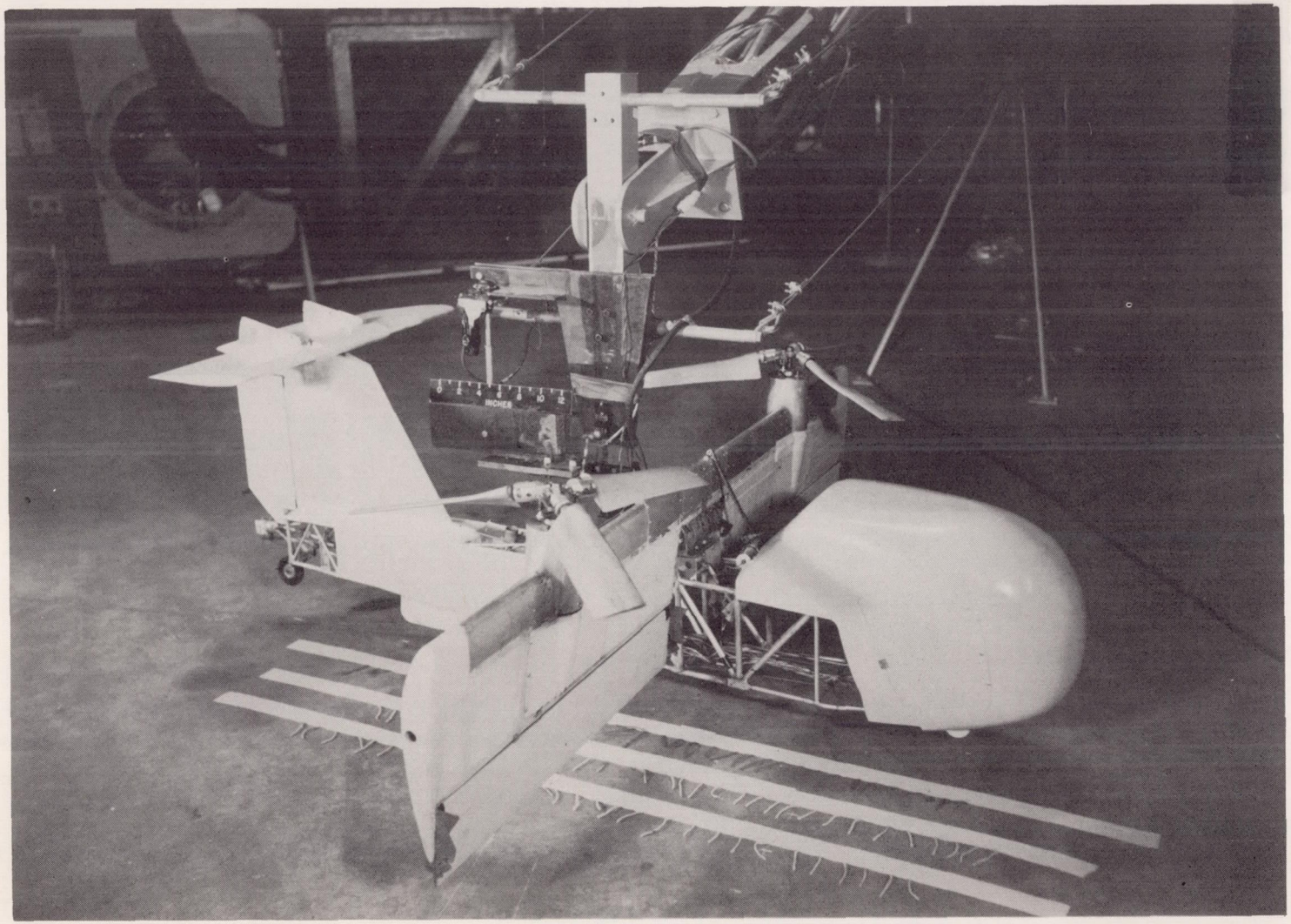

L-60-5430

Figure 2.- Photograph of installation similar to setup used in the tests.

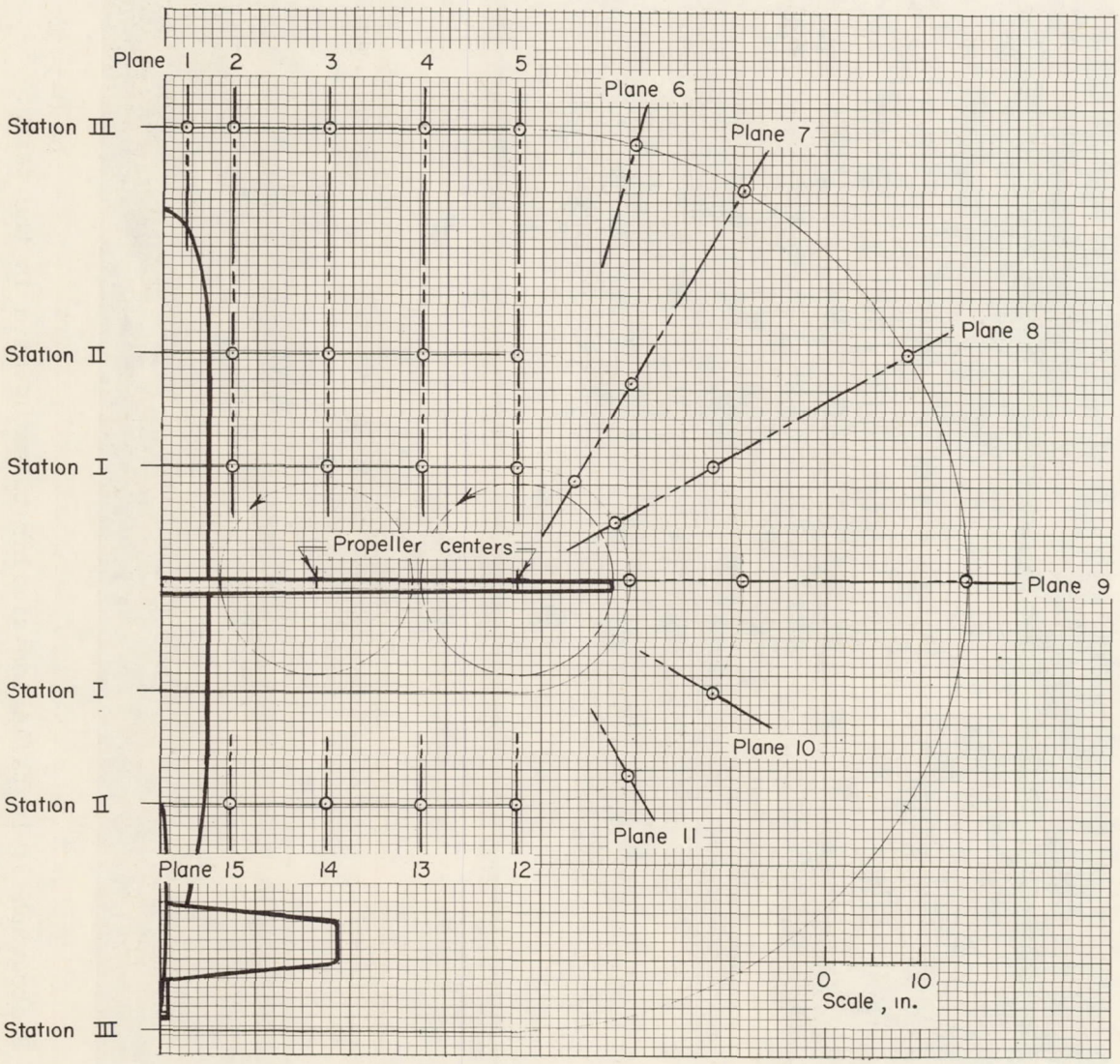

(a) Four-propeller model.

Figure 3.- Survey stations around the models.

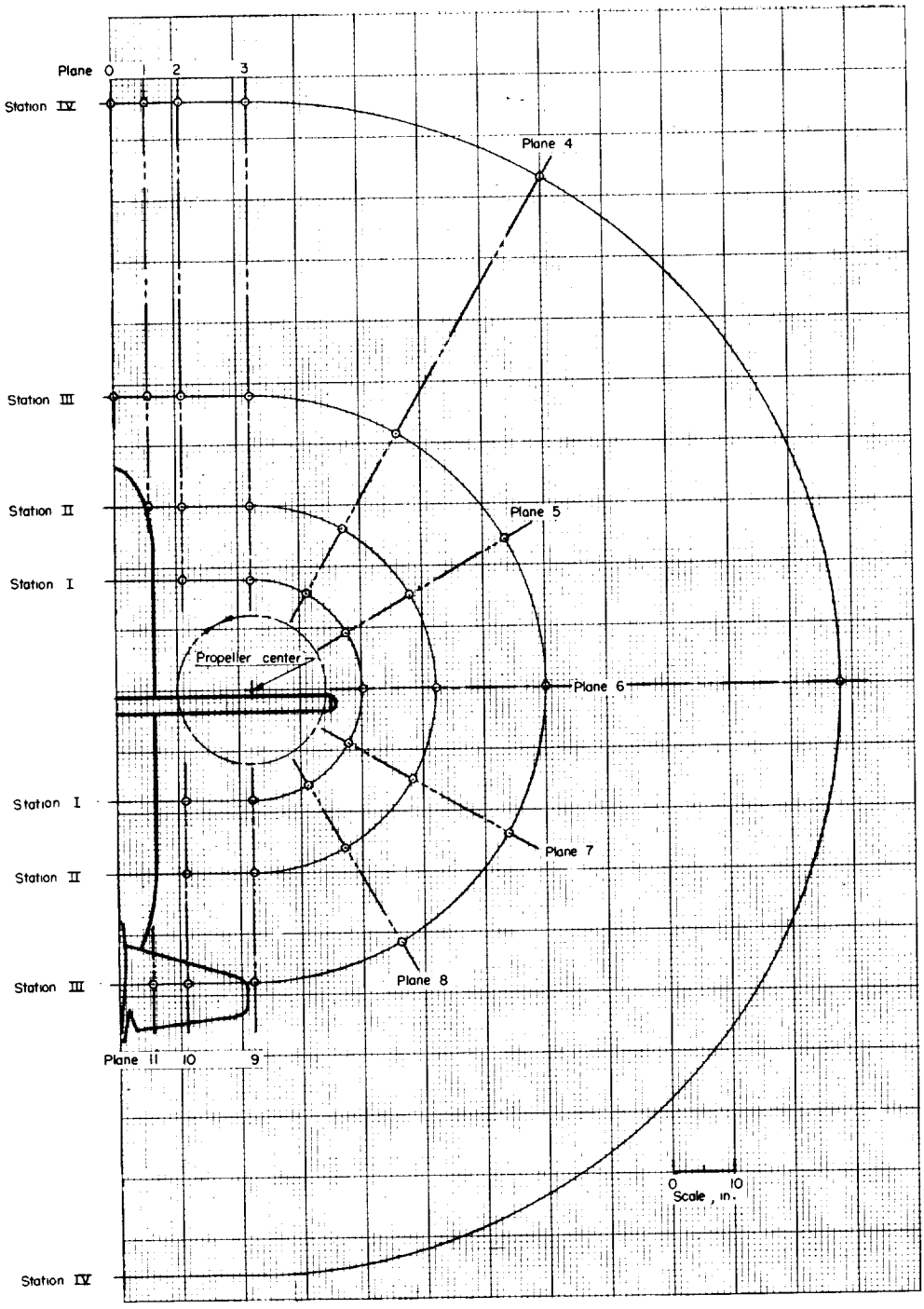

(b) Hiller X-18 model.

Figure 3.- Continued.

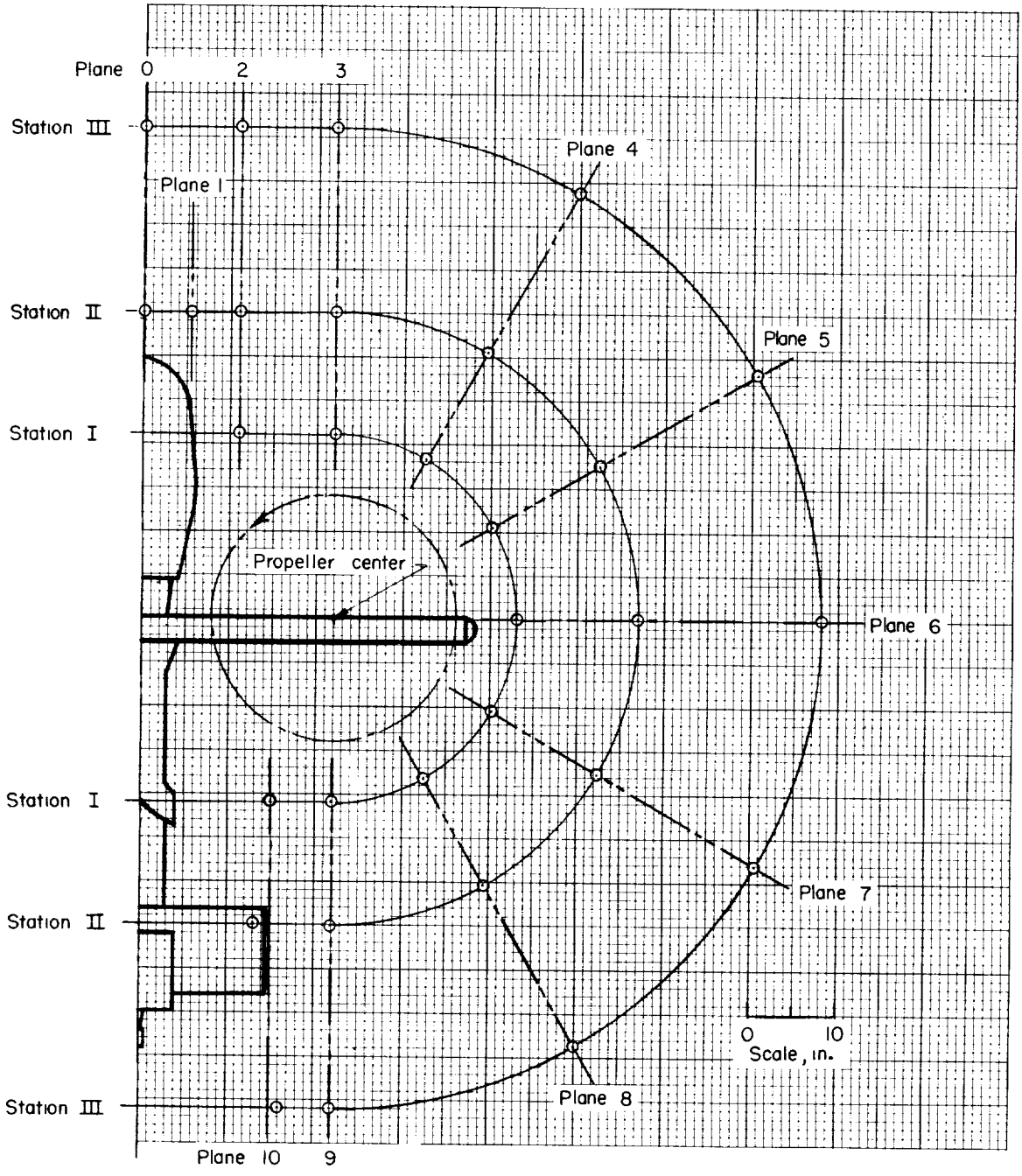

(c) VZ-2 model.

Figure 3.- Concluded.

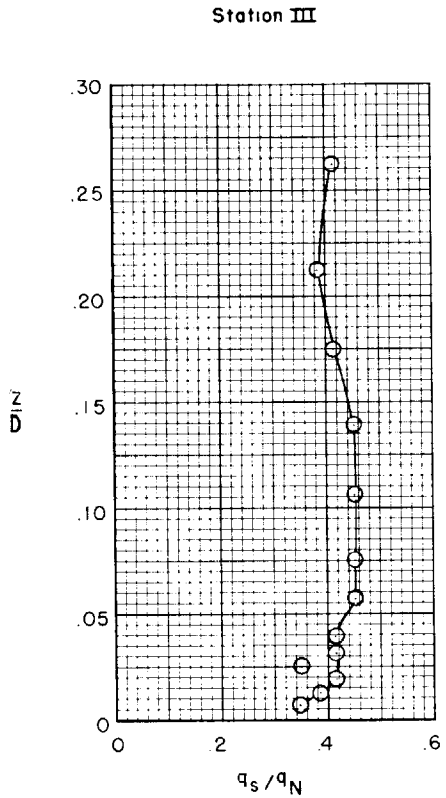

(a) Plane 1.

Figure 4.- Dynamic-pressure profiles measured with the four-propeller model. h/D = 1.5; q_N = 6 lb/sq ft.

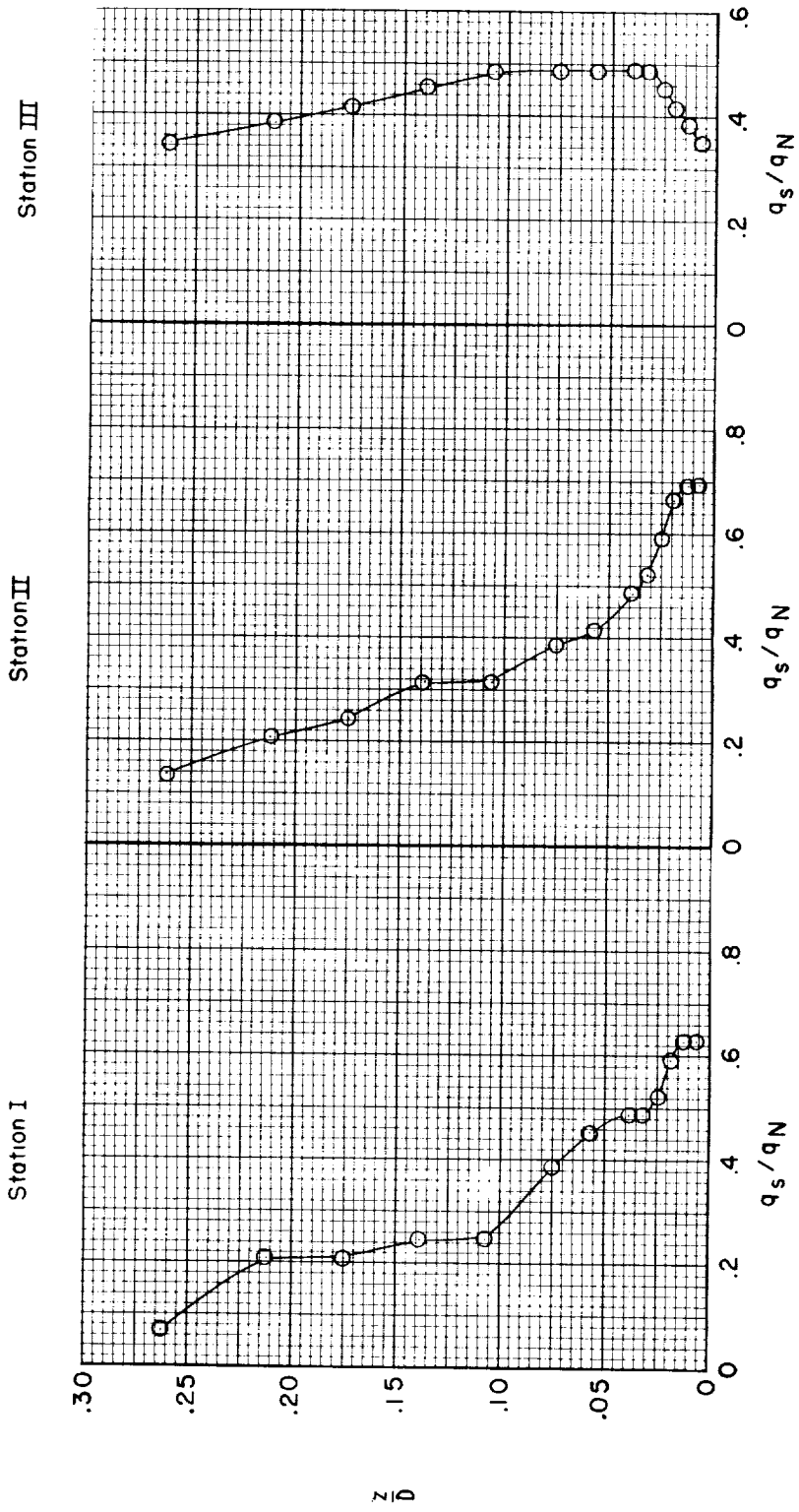

(b) Plane 2.

Figure 4.- Continued.

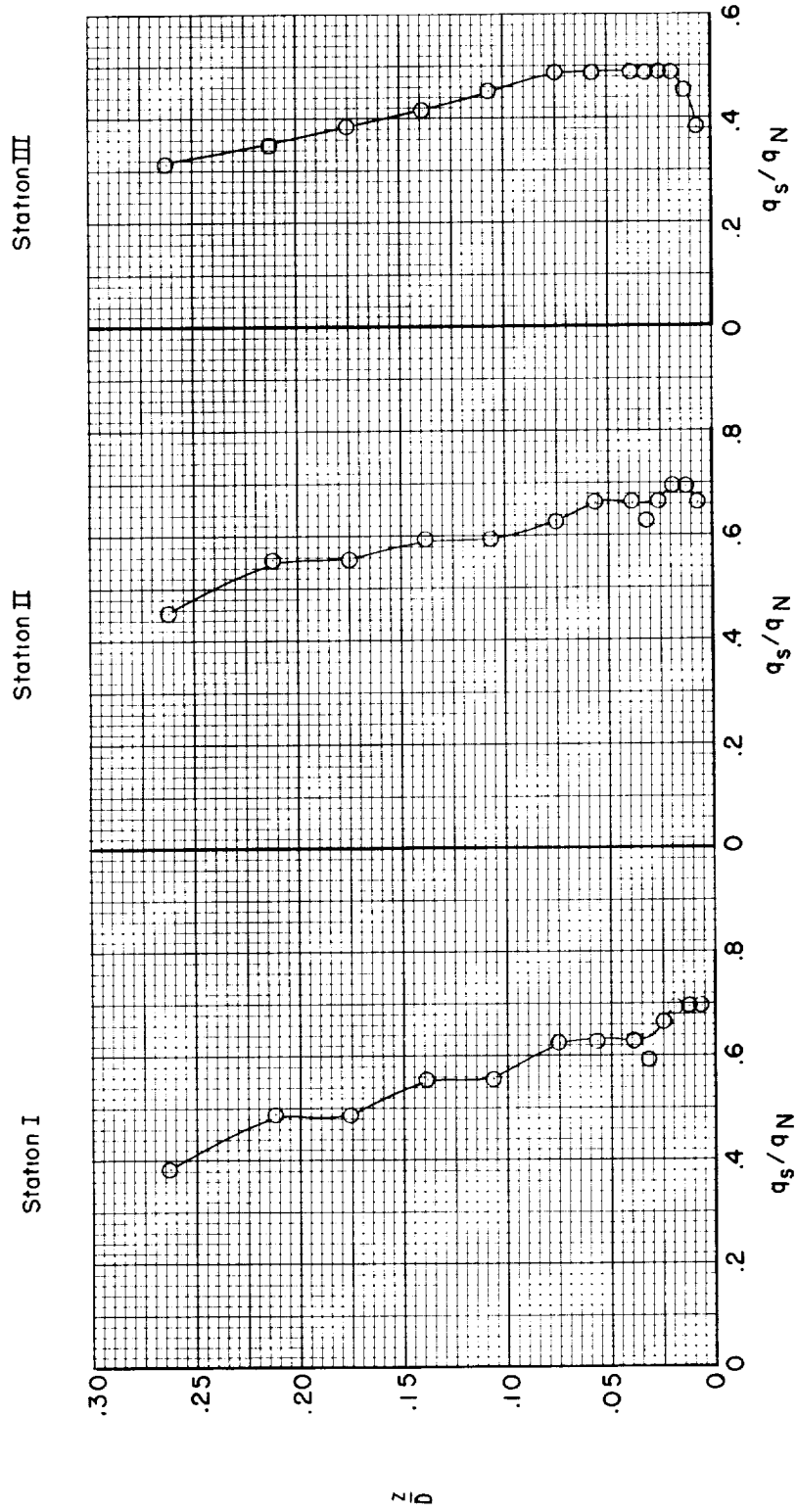

(c) Plane 3.

Figure 4.- Continued.

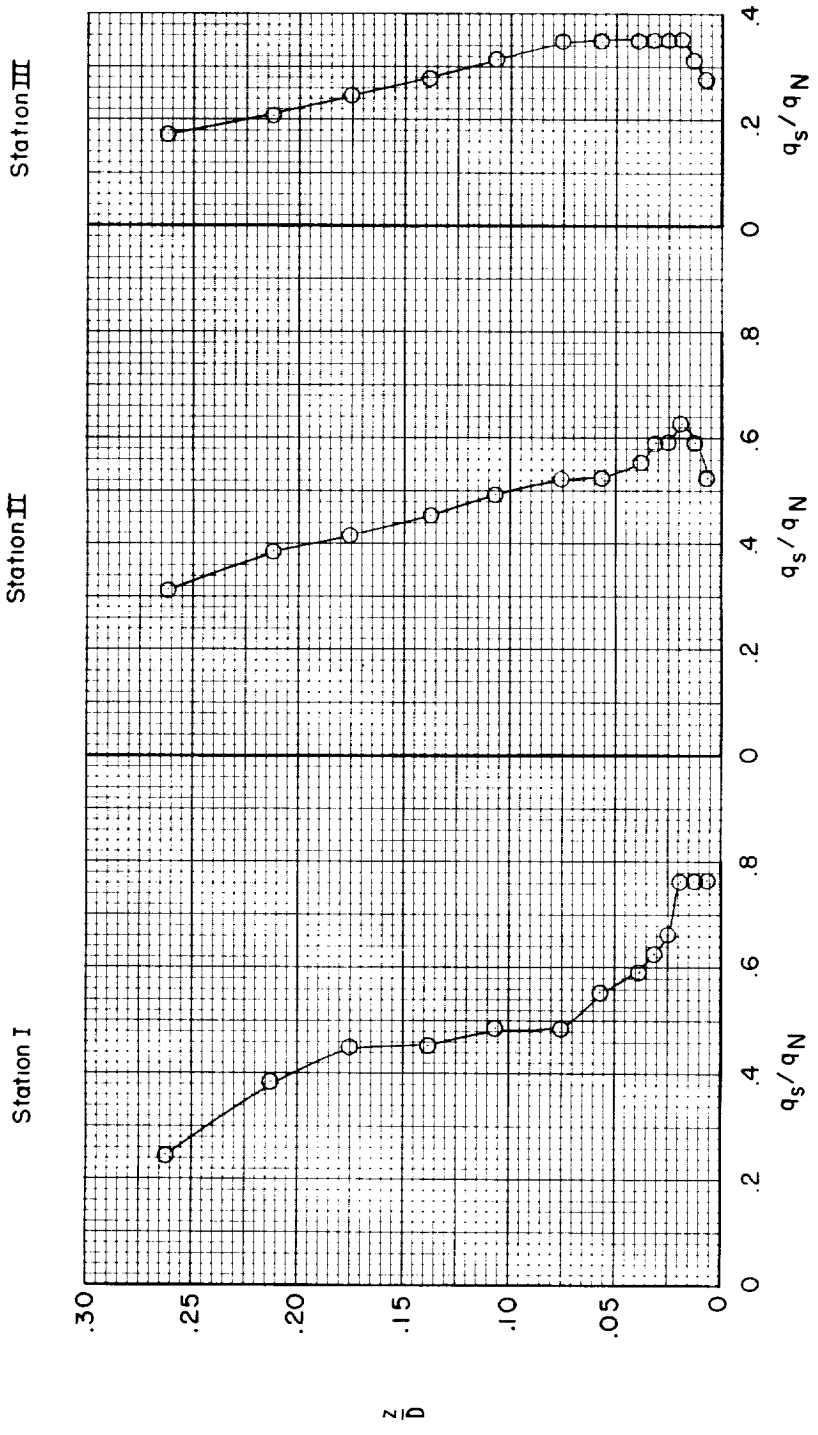

(d) Plane 4.

Figure 4.- Continued.

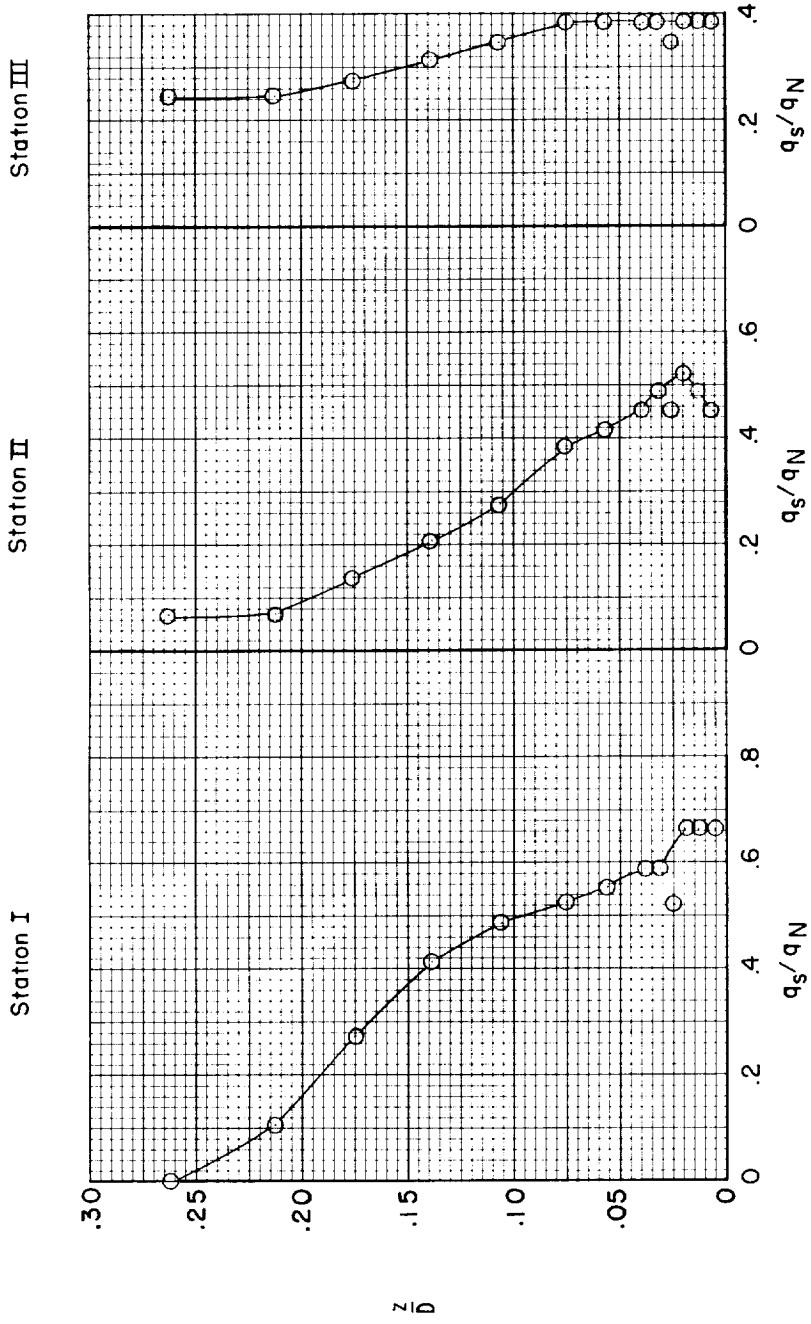

(e) Plane 5.

Figure 4.- Continued.

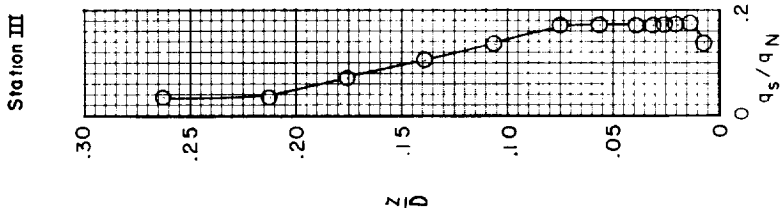

(f) Plane 6.

Figure 4.- Continued.

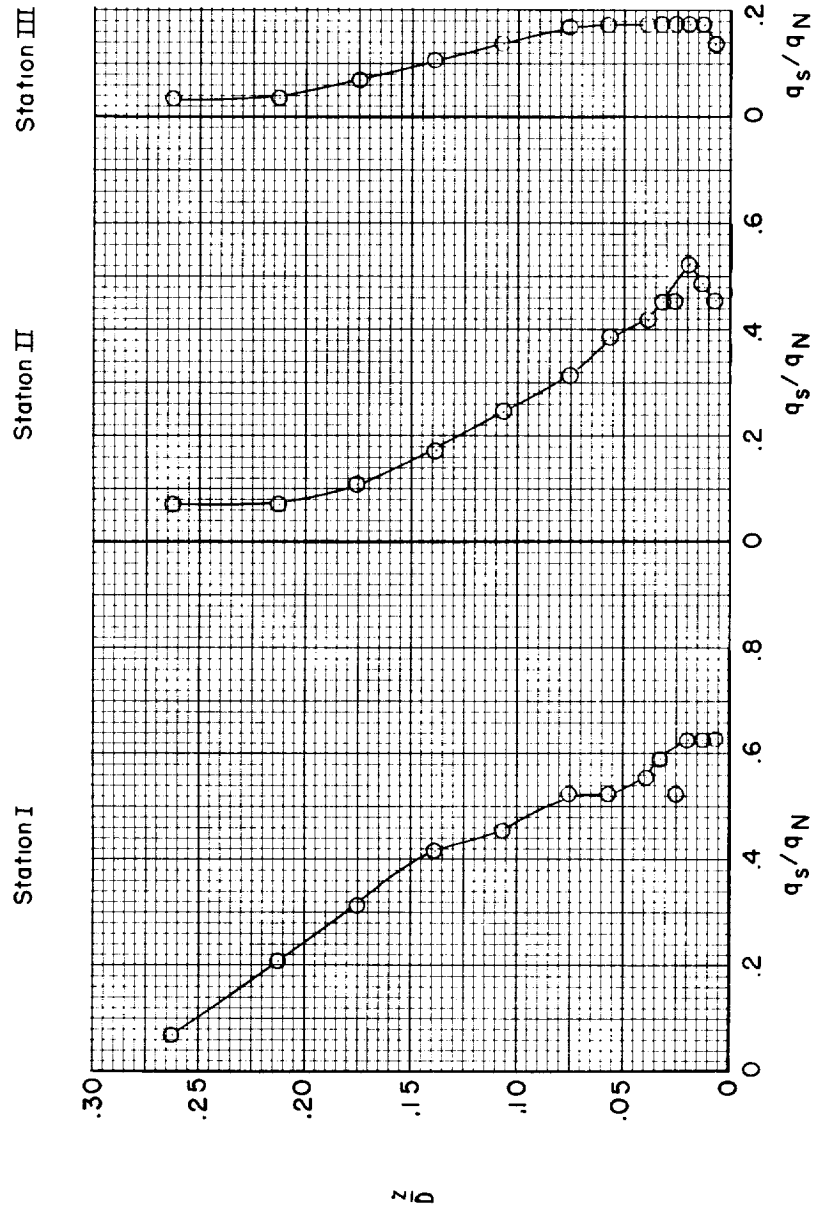

(g) Plane 7.

Figure 4.- Continued.

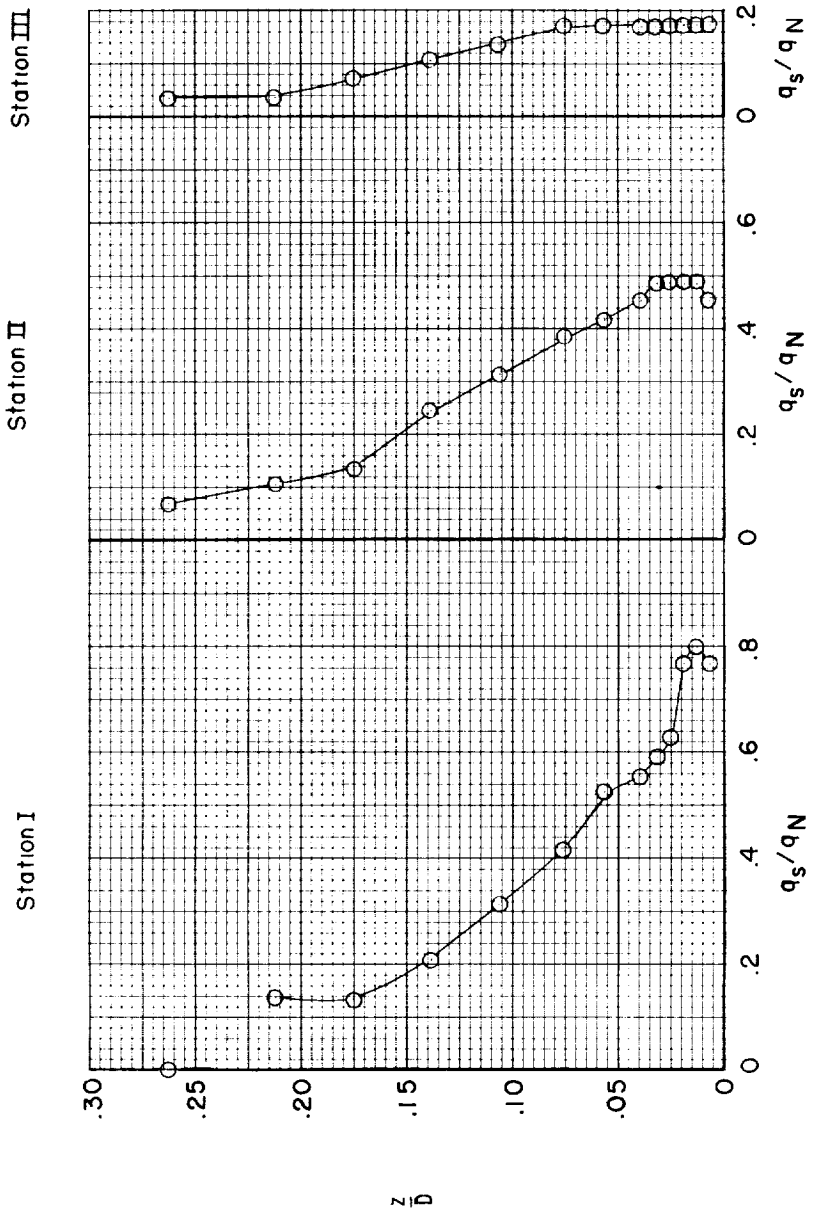

(h) Plane 8.

Figure 4.- Continued.

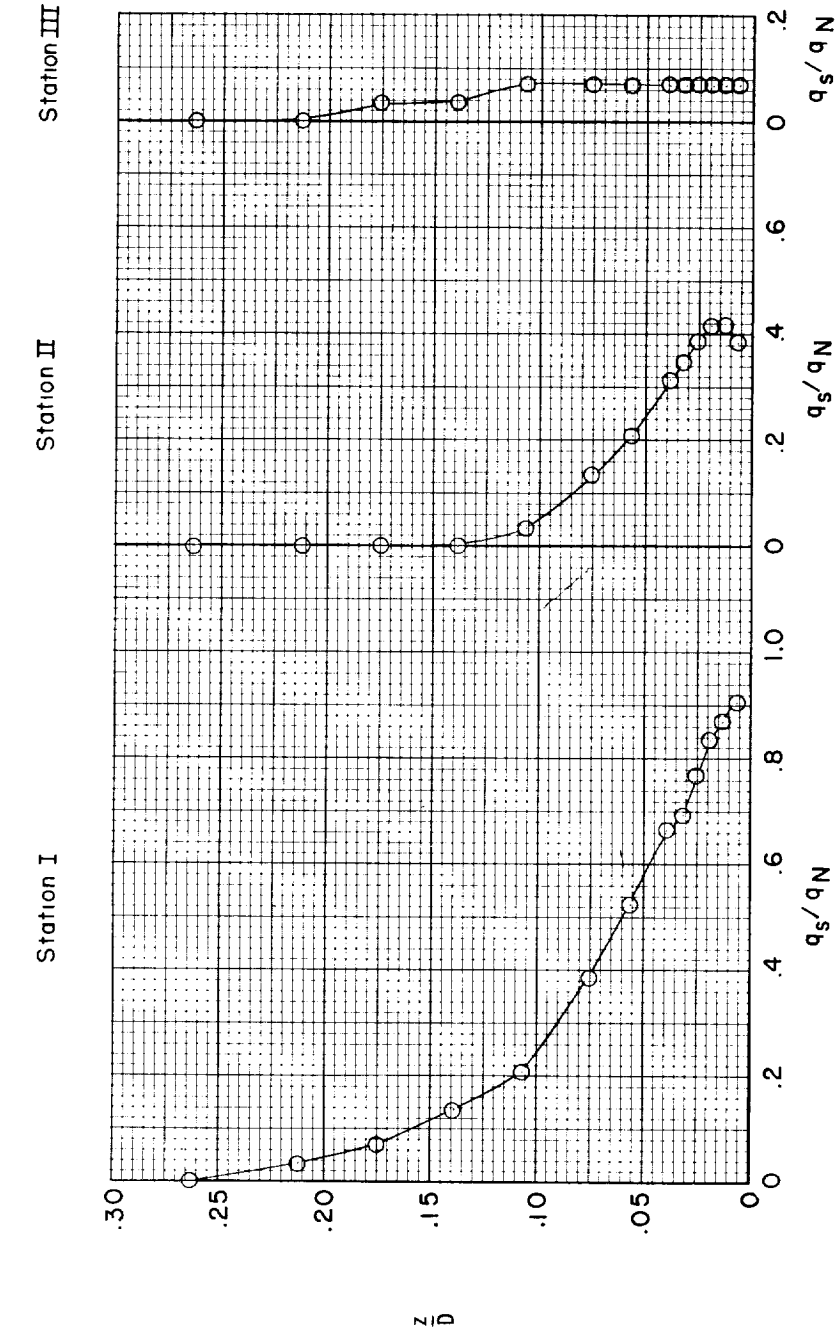

(i) Plane 9.

Figure 4.- Continued.

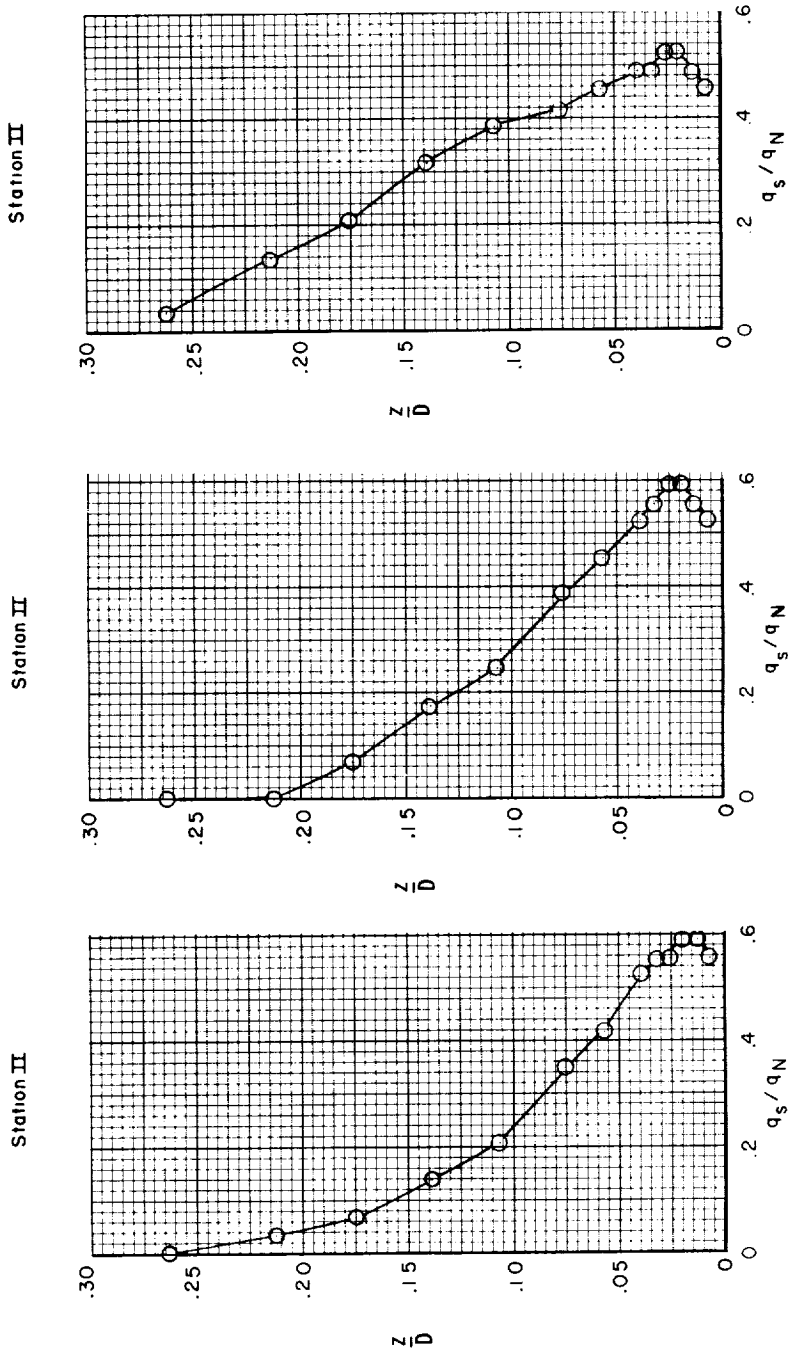

(j) Plane 10.

(k) Plane 11.

(l) Plane 12.

Figure 4.- Continued.

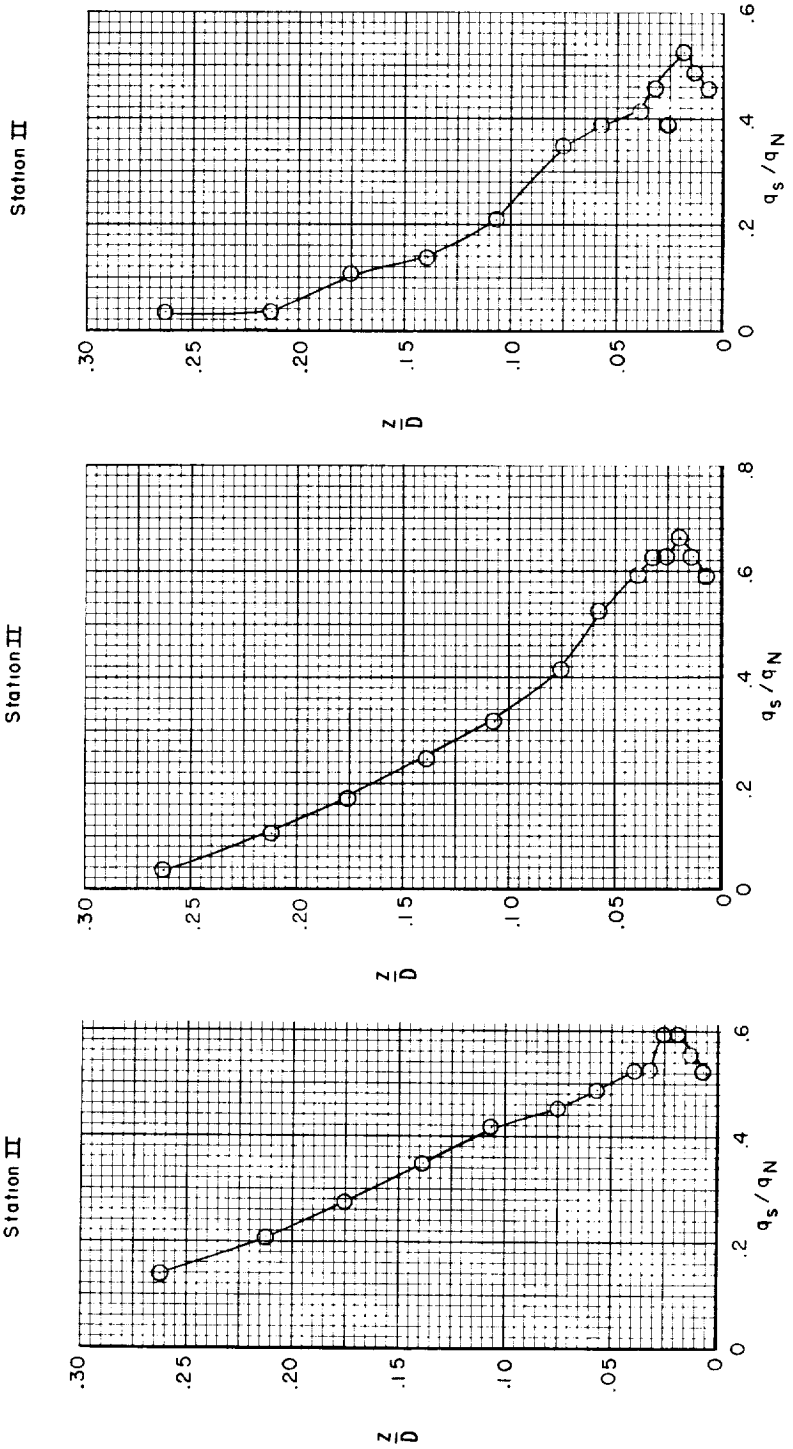

(m) Plane 13.

(n) Plane 14.

(o) Plane 15.

Figure 4.- Concluded.

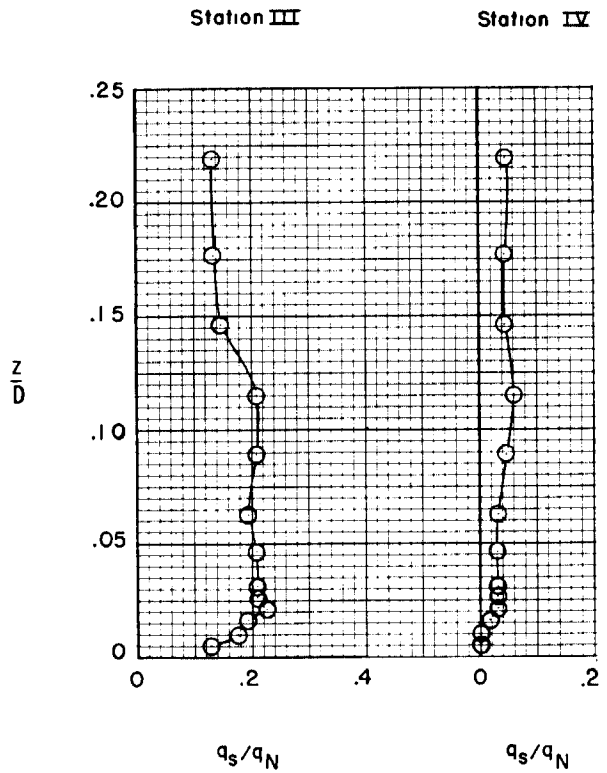

(a) Plane 0.

Figure 5.- Dynamic-pressure profiles measured with the Hiller X-18 model. h/D = 1.2; q_N = 7.0 lb/sq ft.

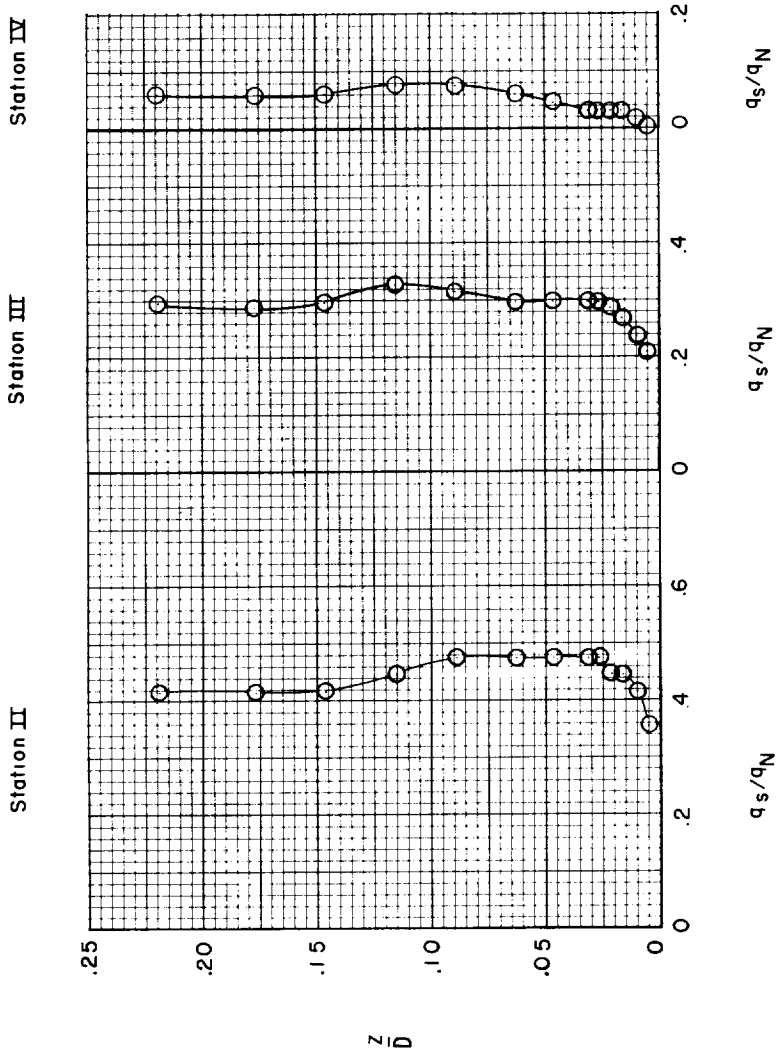

(b) Plane 1.

Figure 5.- Continued.

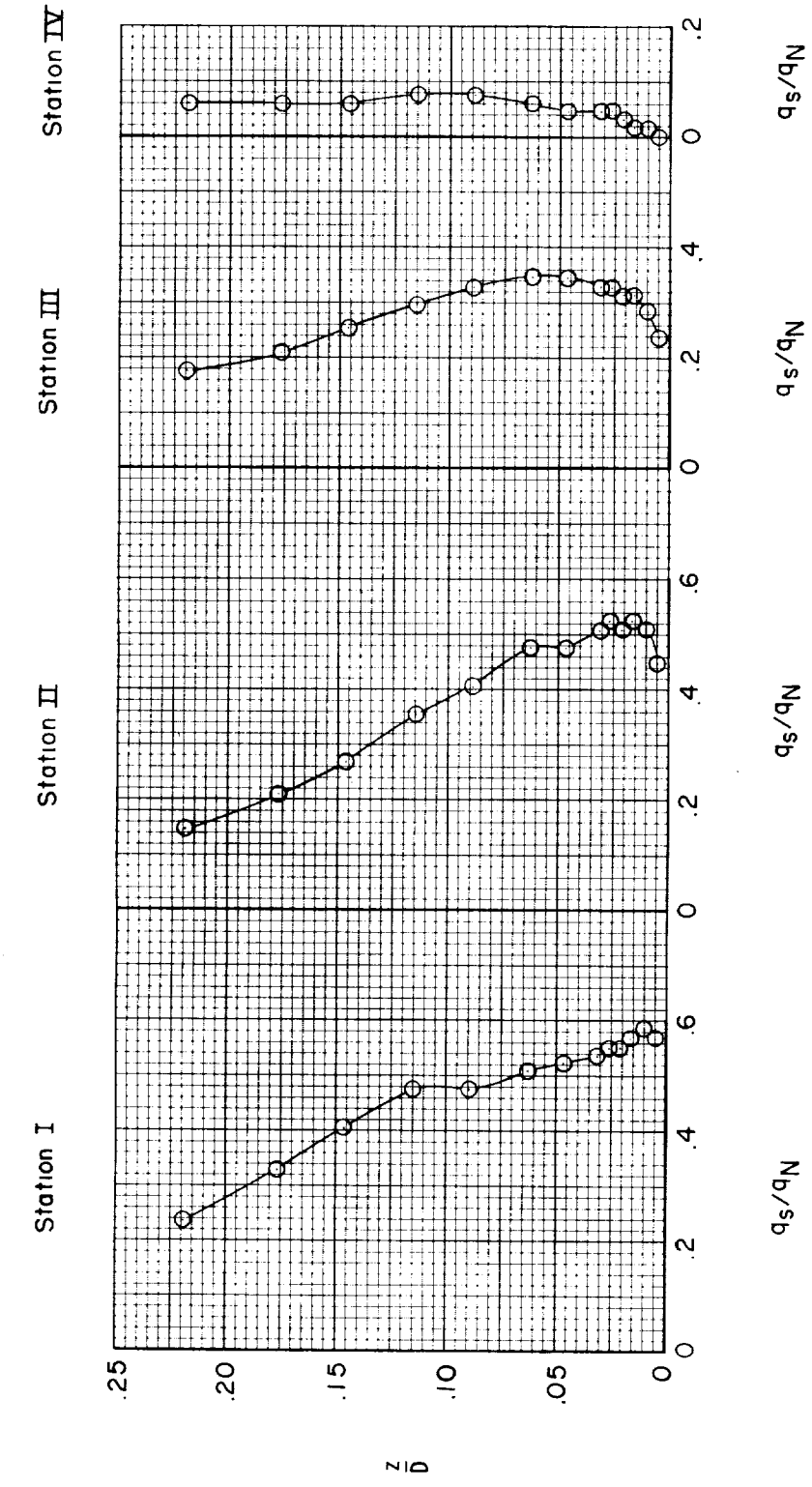

(c) Plane 2.

Figure 5.- Continued.

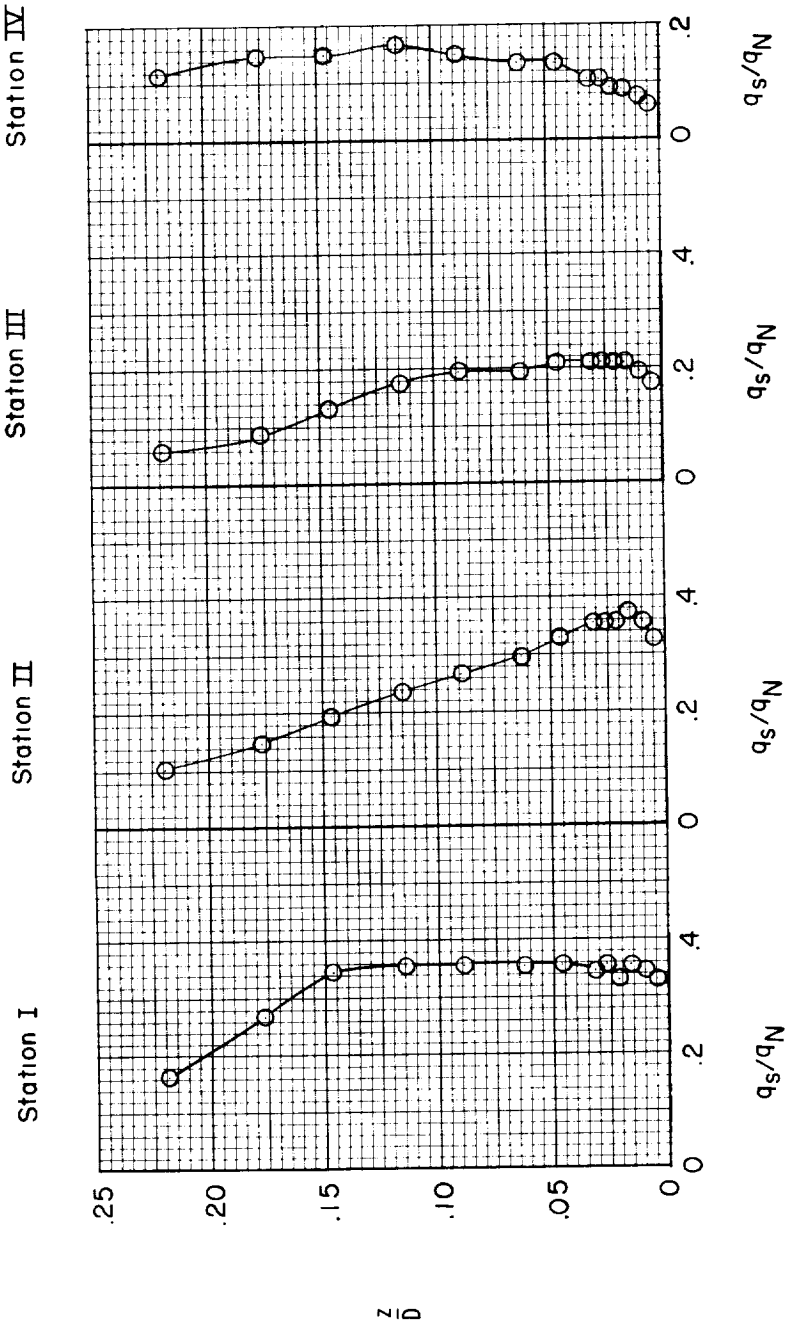

(d) Plane 3.

Figure 5.- Continued.

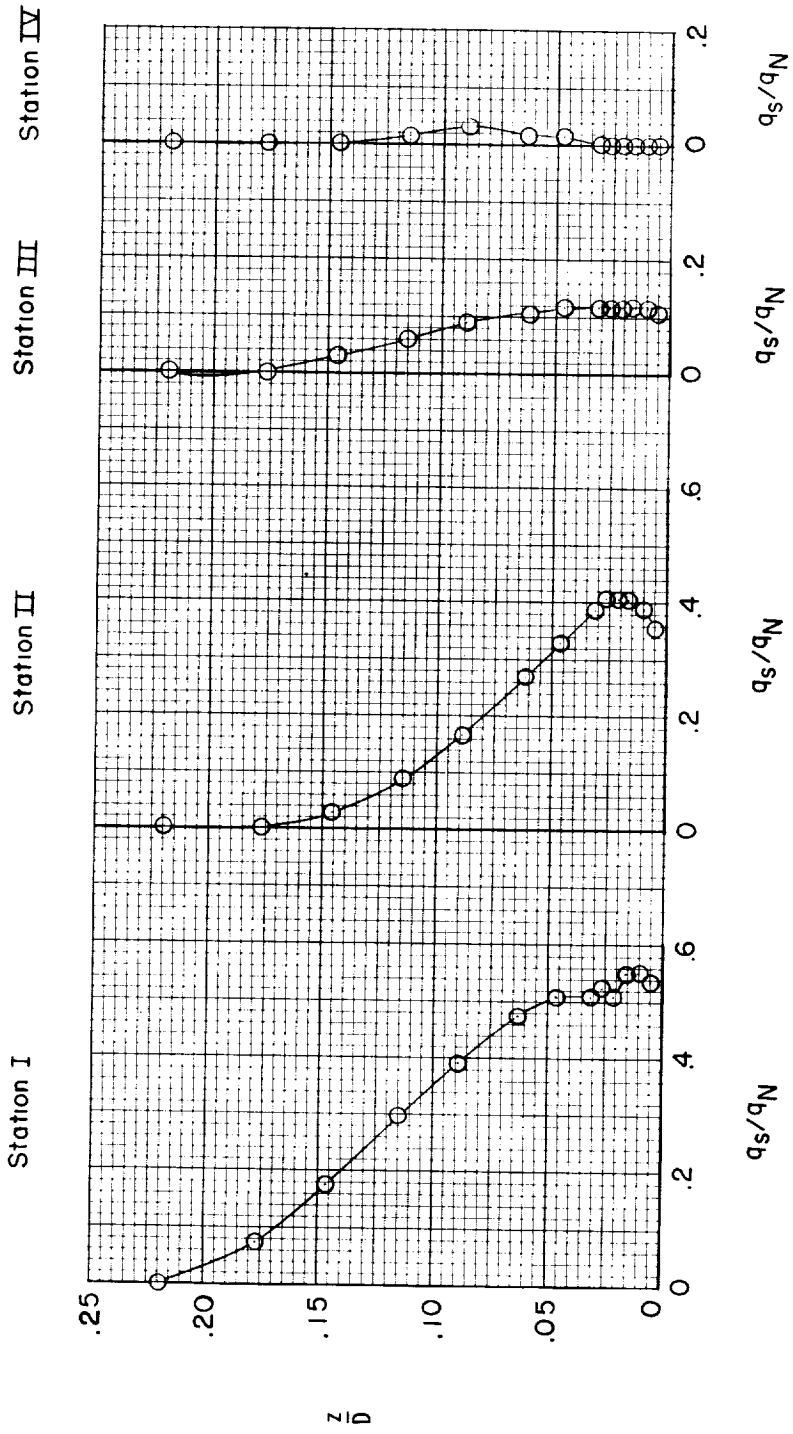

(e) Plane 4.

Figure 5.- Continued.

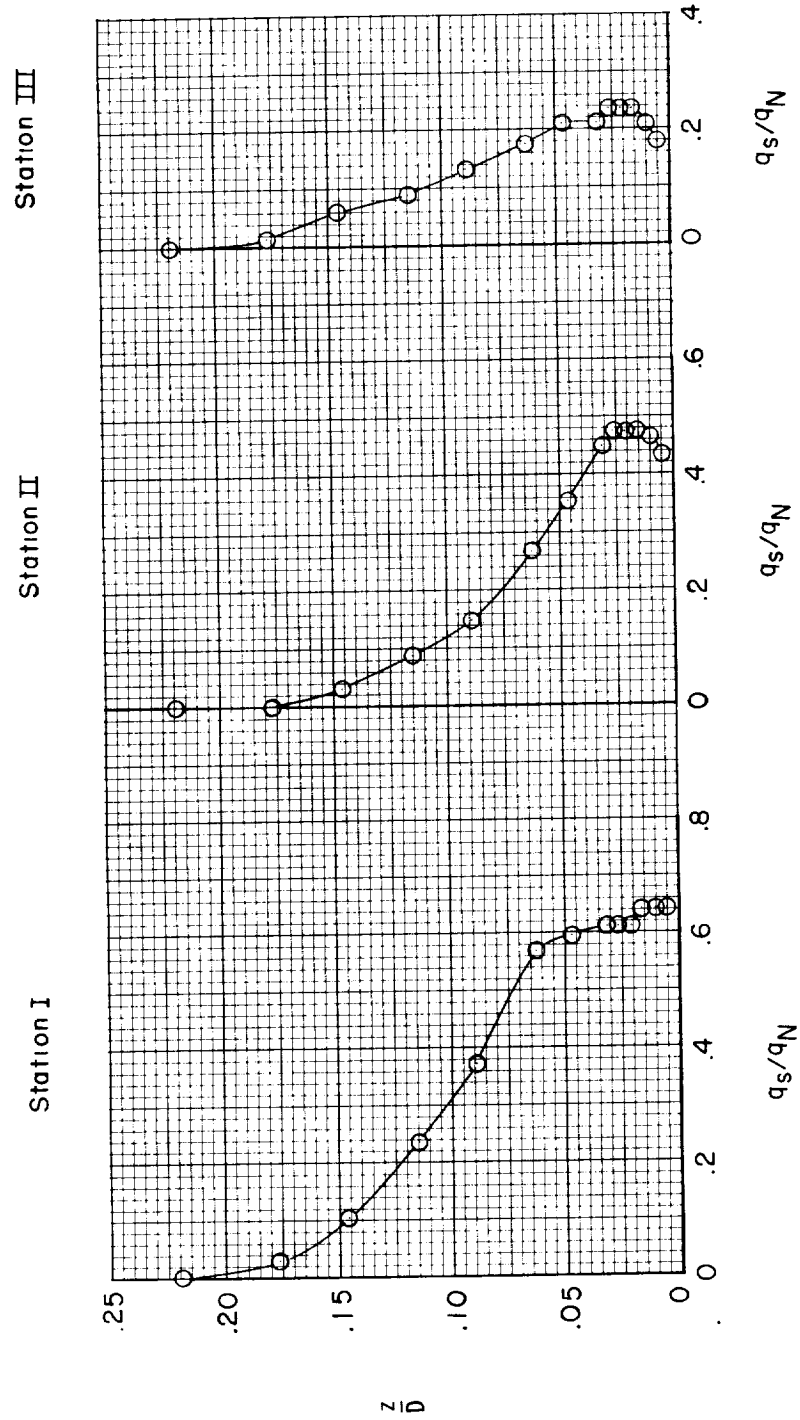

(f) Plane 5.

Figure 5.- Continued.

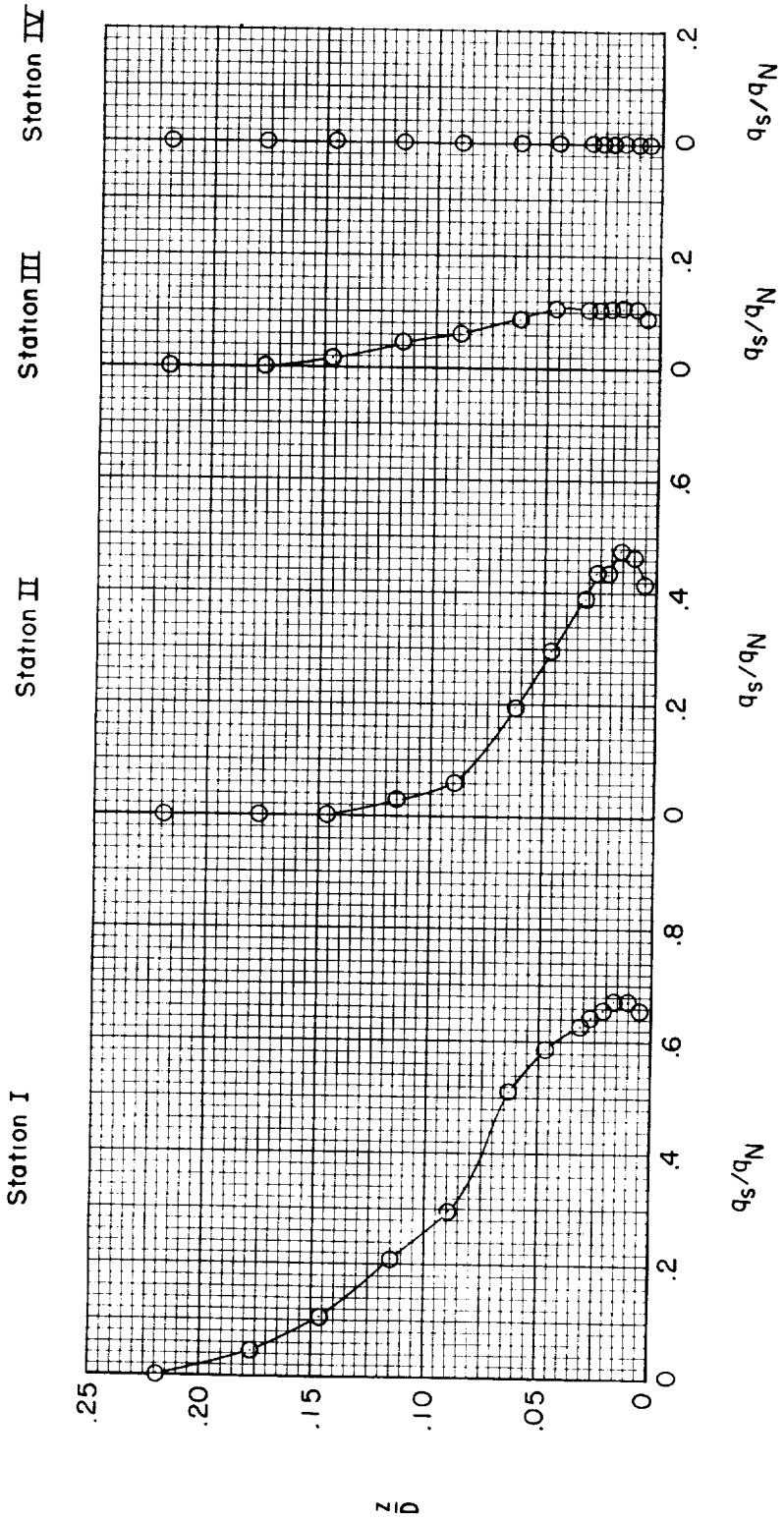

(g) Plane 6.

Figure 5.- Continued.

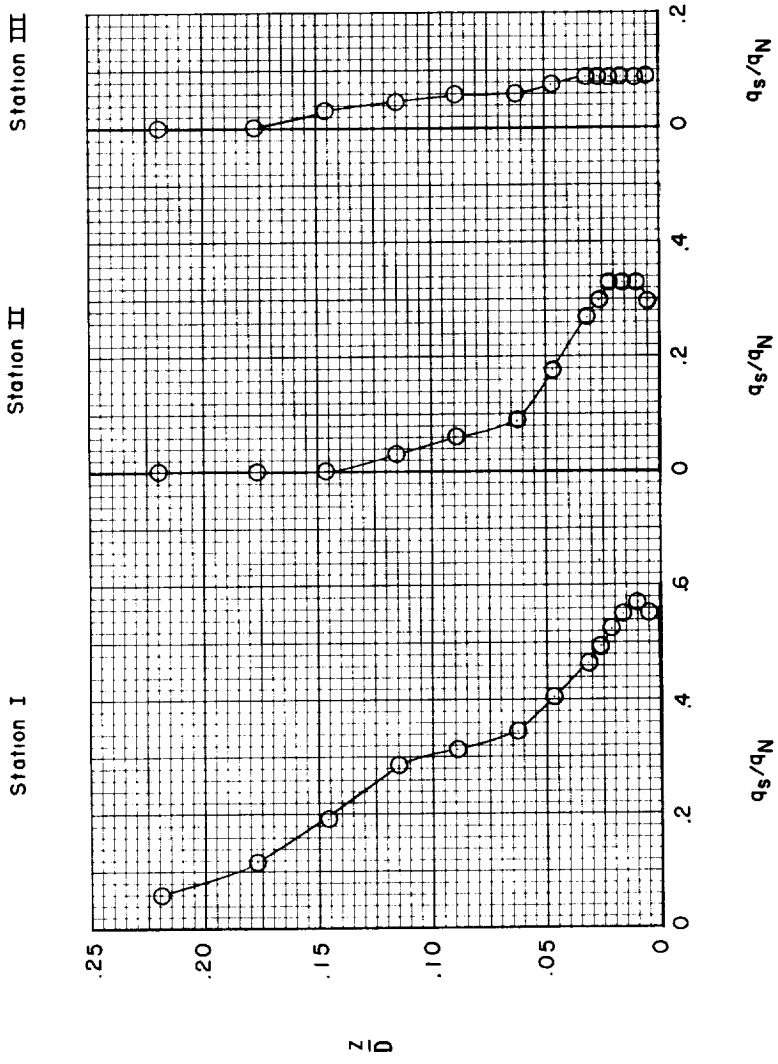

(h) Plane 7.

Figure 5.- Continued.

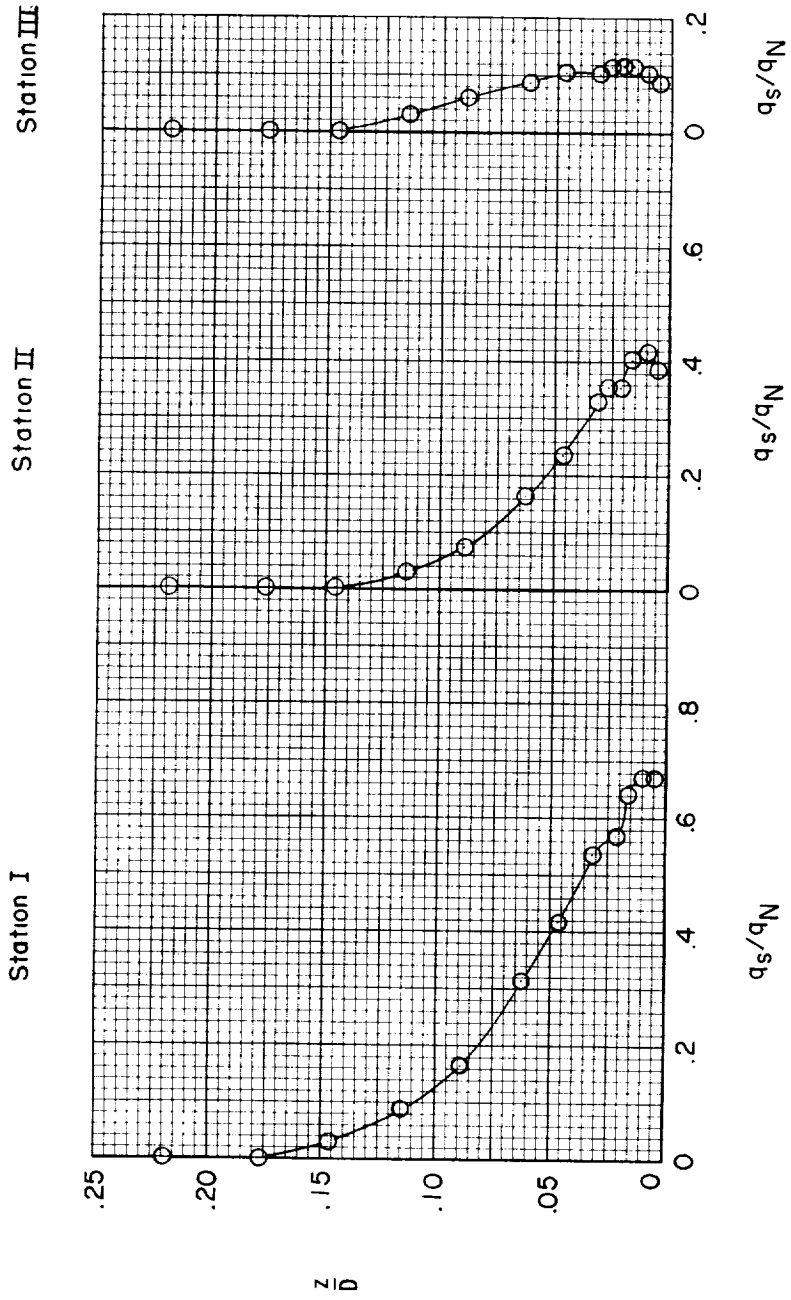

(i) Plane 8.

Figure 5.- Continued.

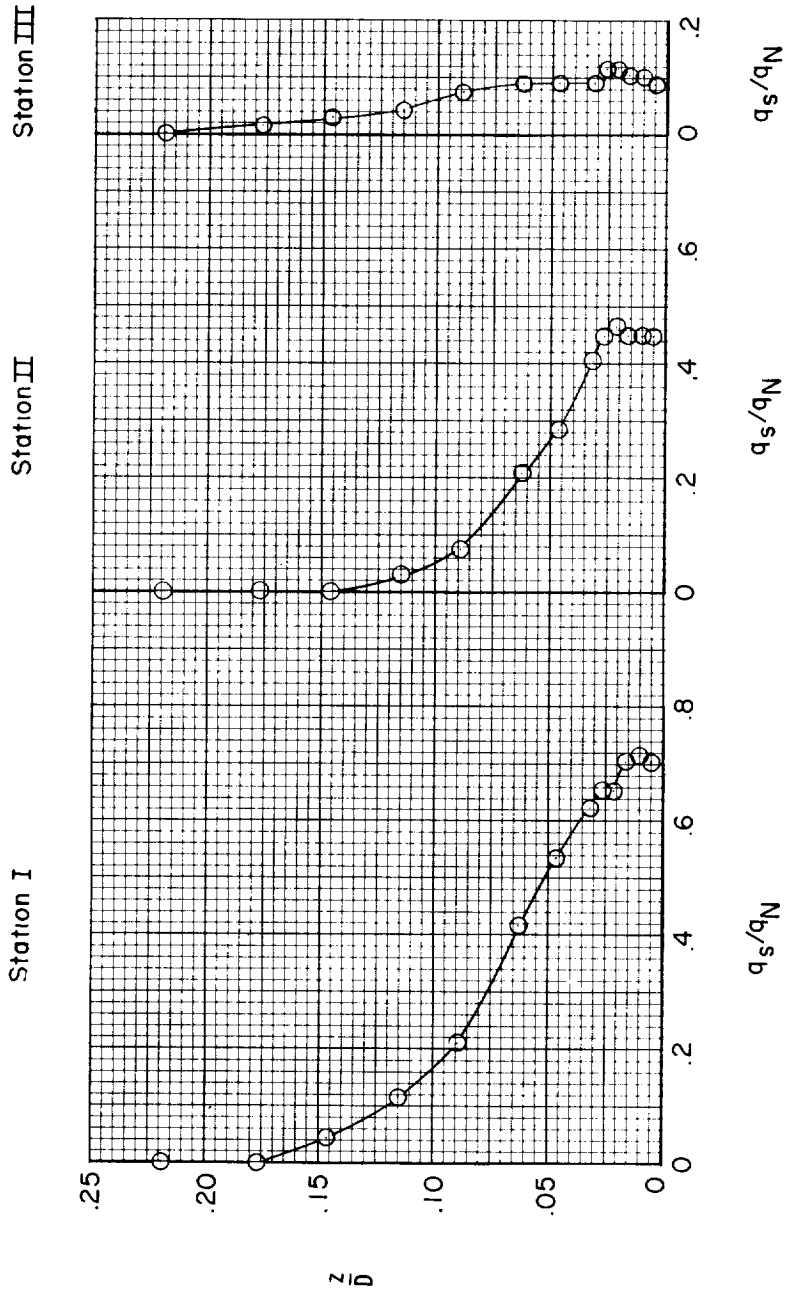

(j) Plane 9.

Figure 5.- Continued.

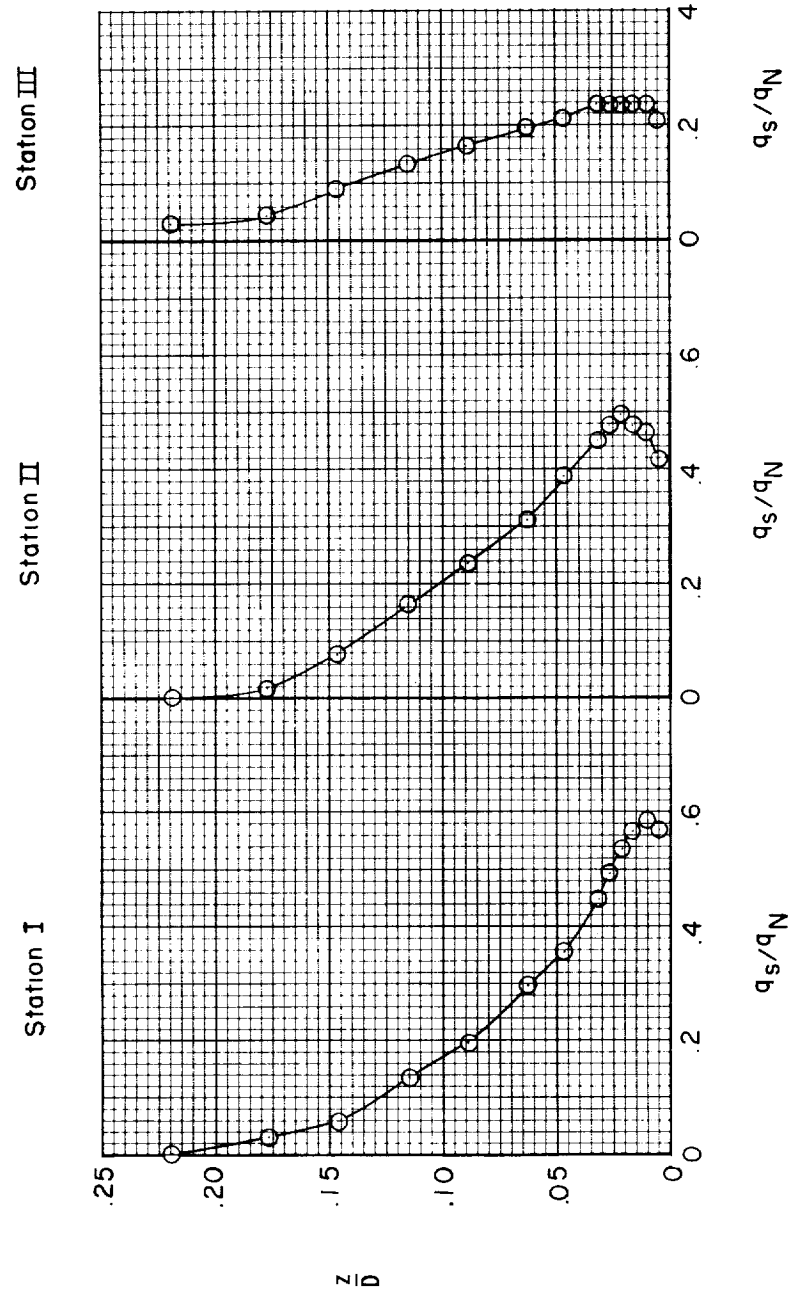

(k) Plane 10.

Figure 5.- Continued.

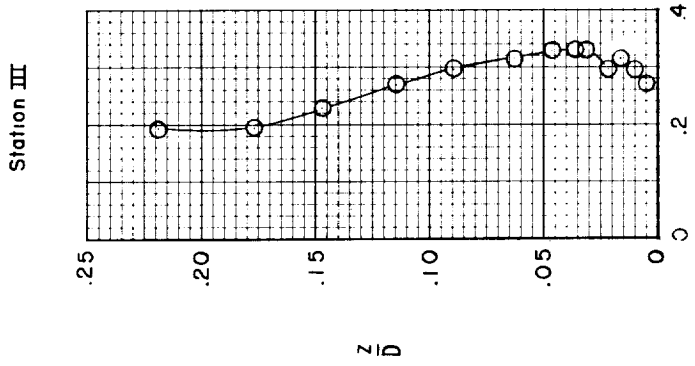

(l) Plane 11.

Figure 5.- Concluded.

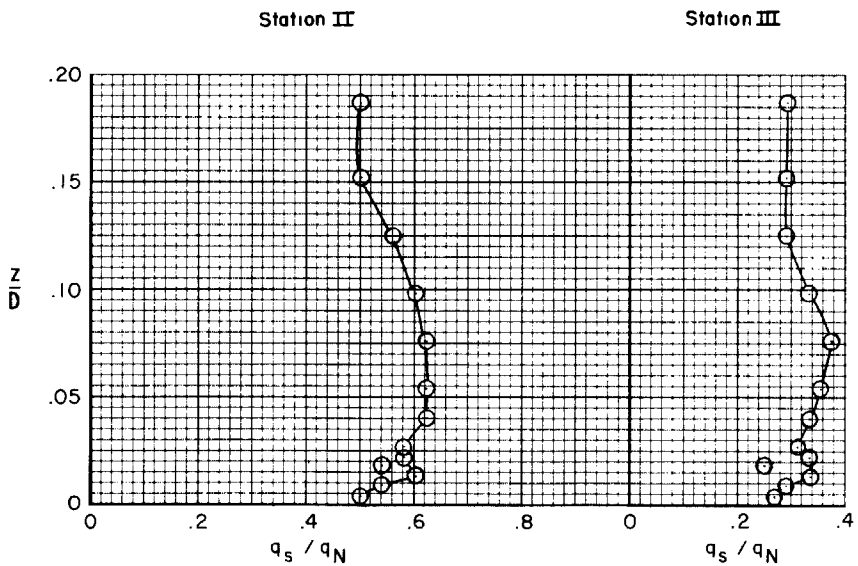

(a) Plane 0.

Figure 6.- Dynamic-pressure profiles measured with the VZ-2 model. h/D = 1.1; q_N = 5.0 lb/sq ft.

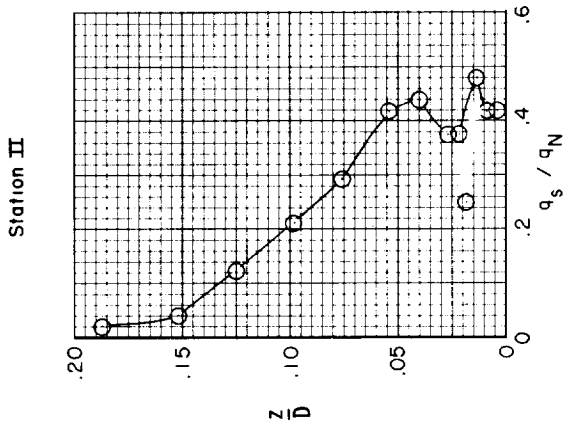

(b) Plane 1.

Figure 6.- Continued.

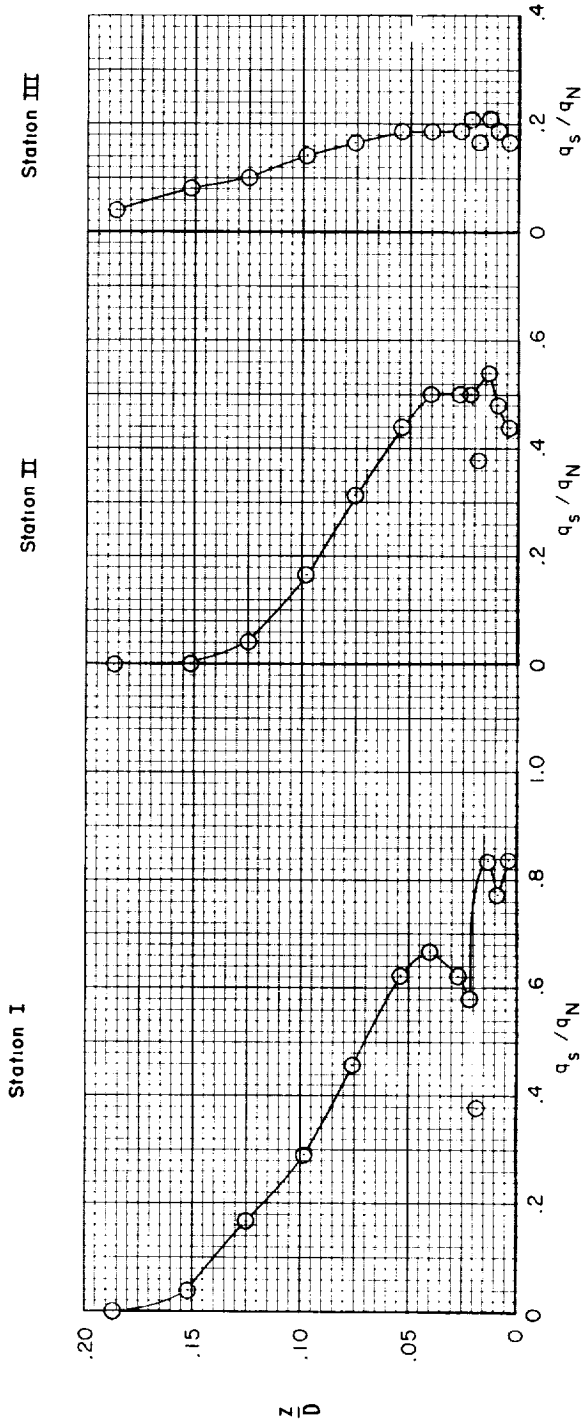

(c) Plane 2.

Figure 6.- Continued.

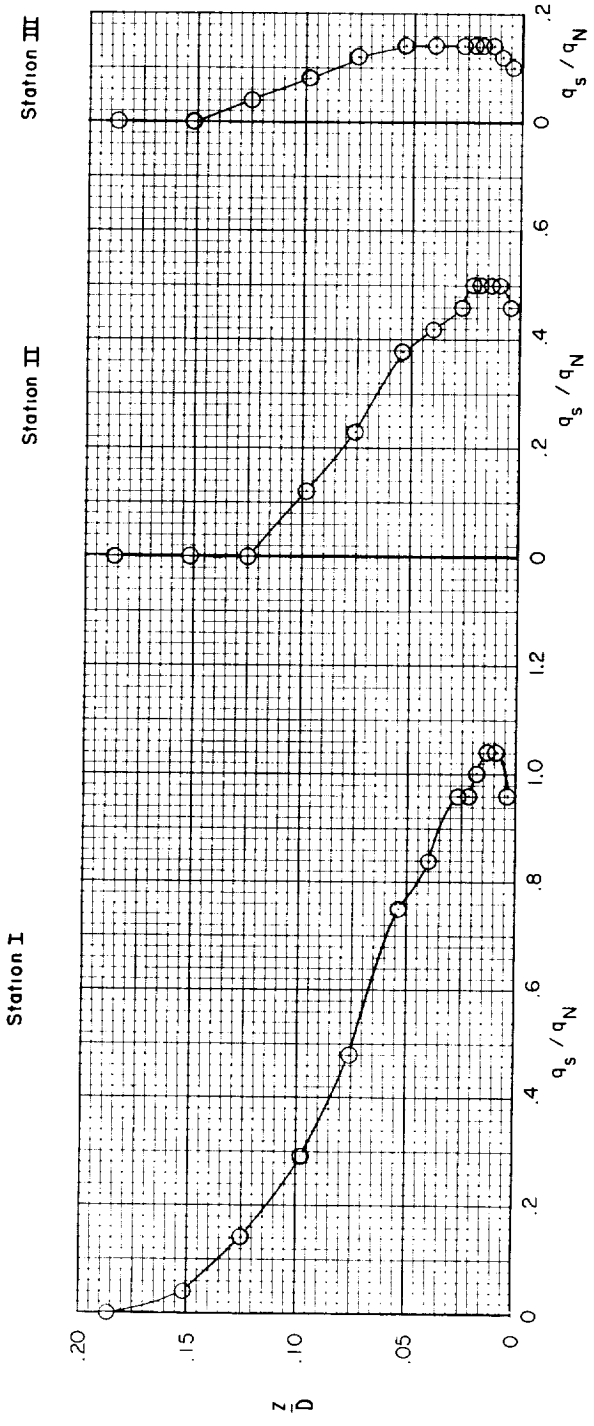

(d) Plane 3.

Figure 6.- Continued.

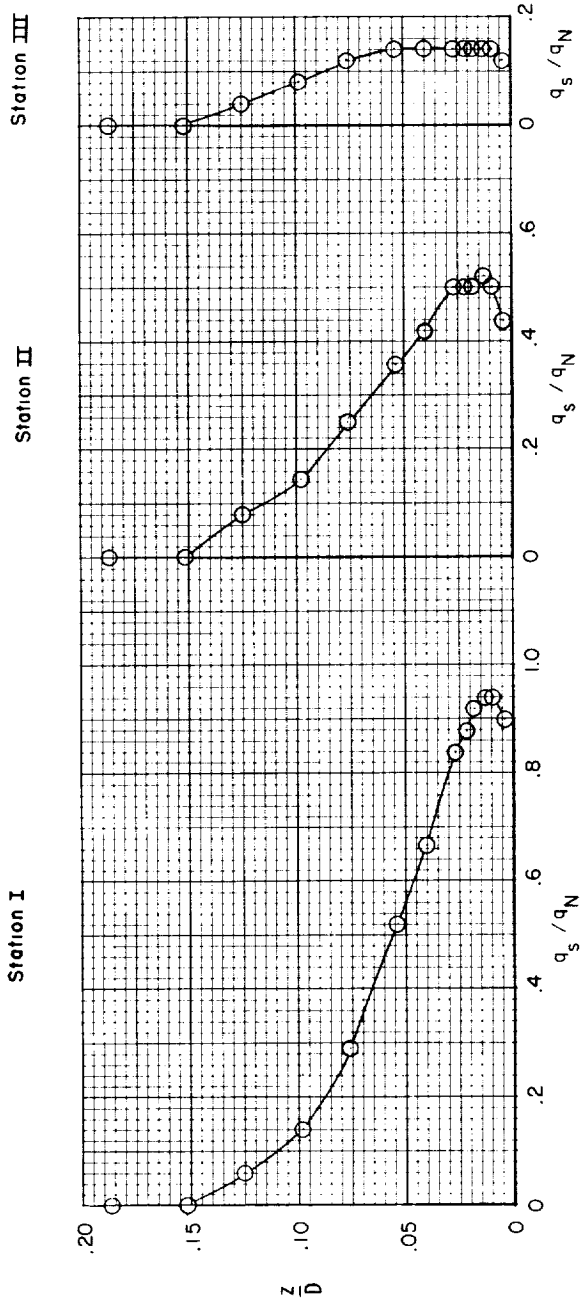

(e) Plane 4.

Figure 6.- Continued.

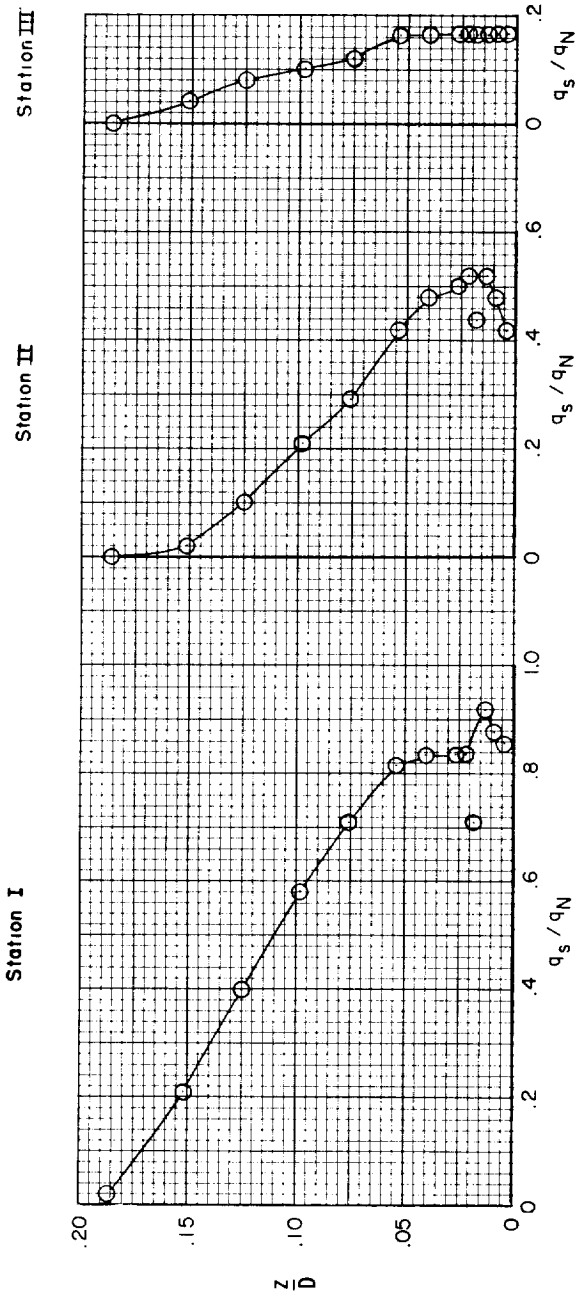

(f) Plane 5.

Figure 6.- Continued.

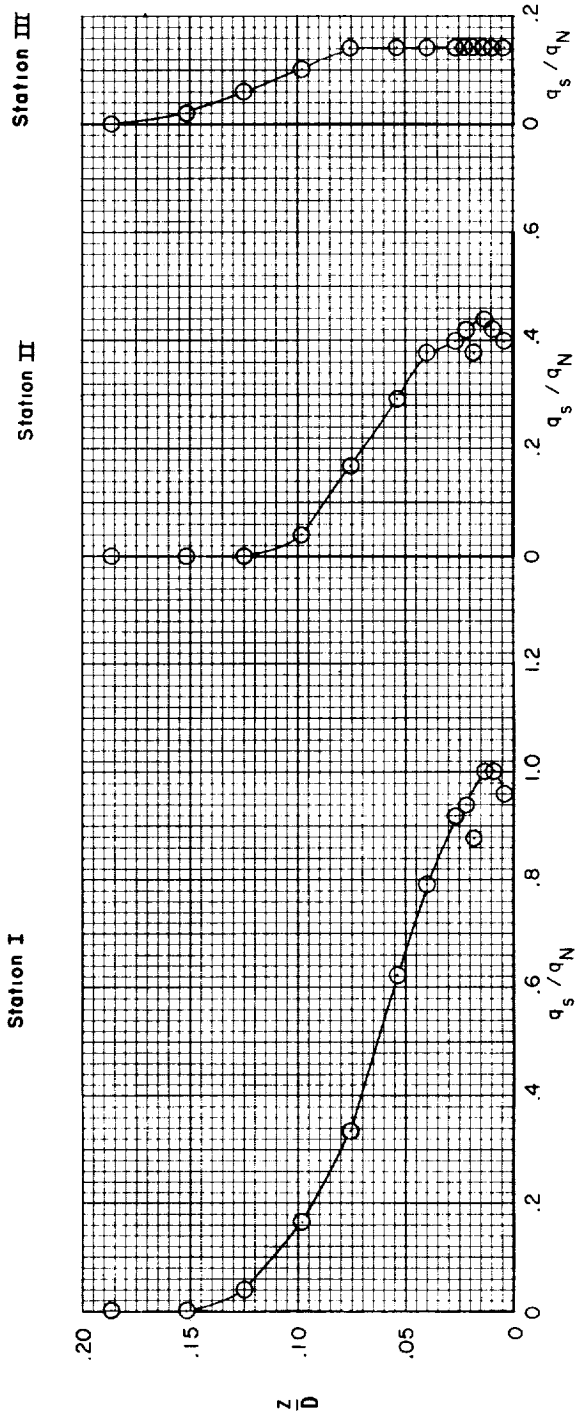

(g) Plane 6.

Figure 6.- Continued.

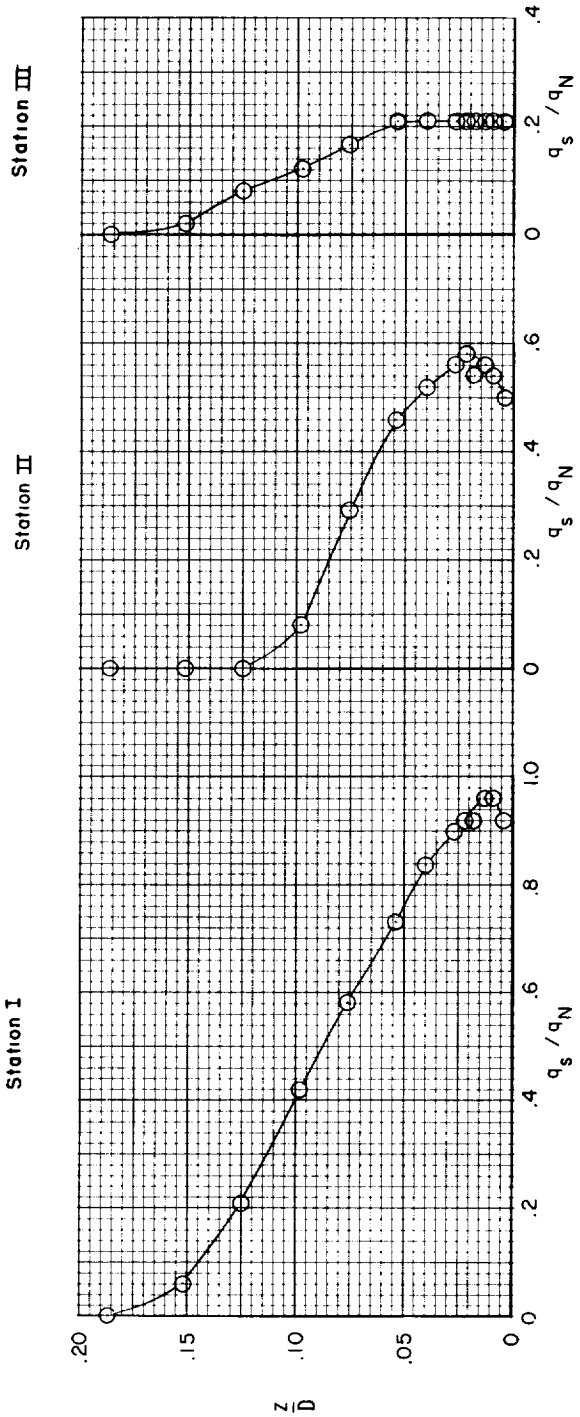

(h) Plane 7.

Figure 6.- Continued.

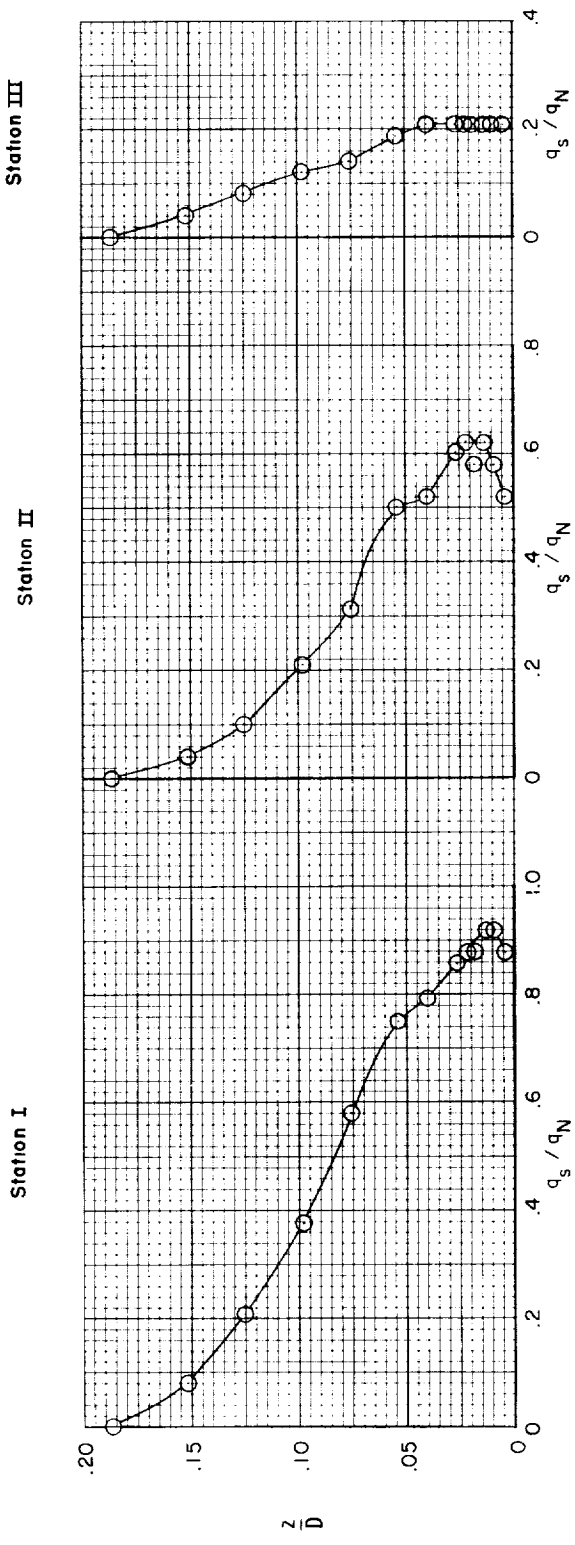

(i) Plane 8.

Figure 6.- Continued.

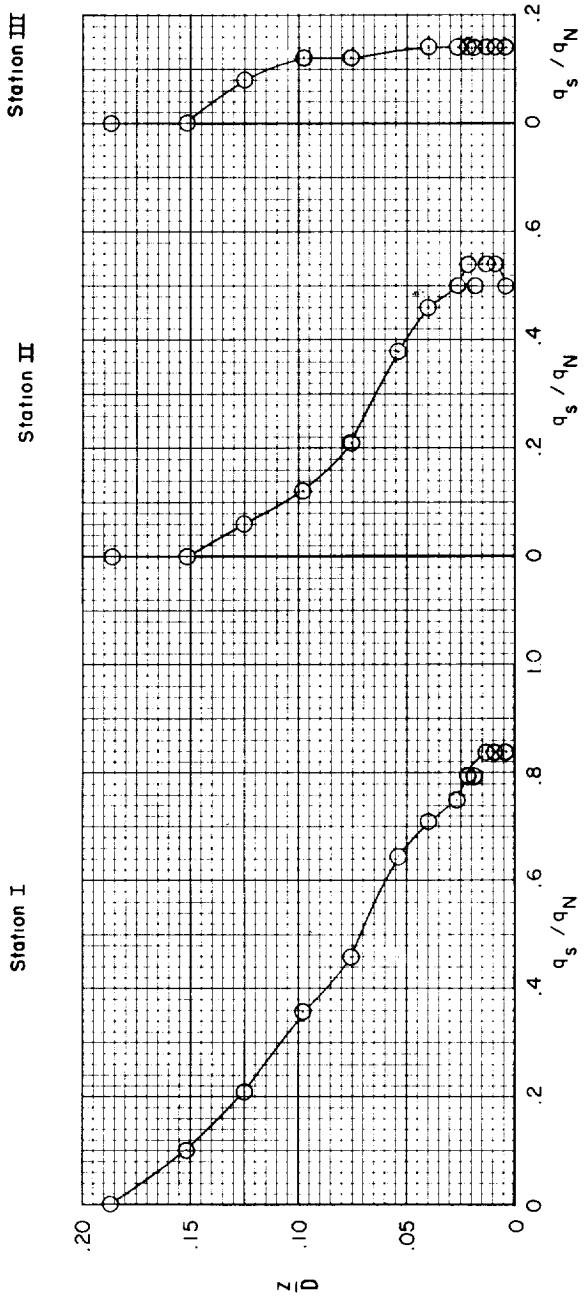

(j) Plane 9.

Figure 6.- Continued.

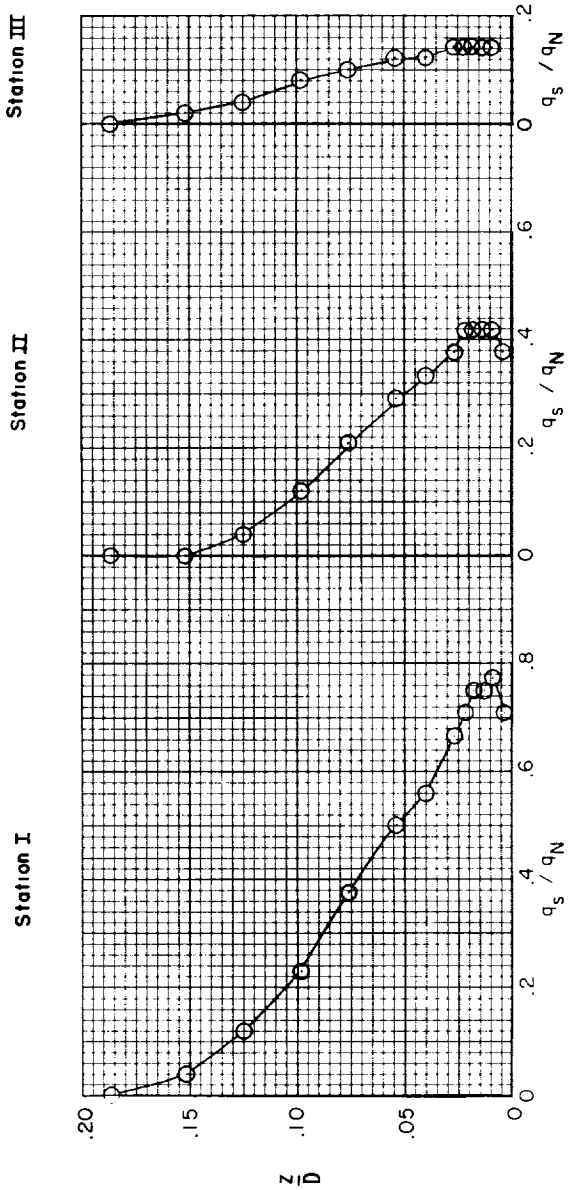

(k) Approximately plane 10.

Figure 6.- Concluded.

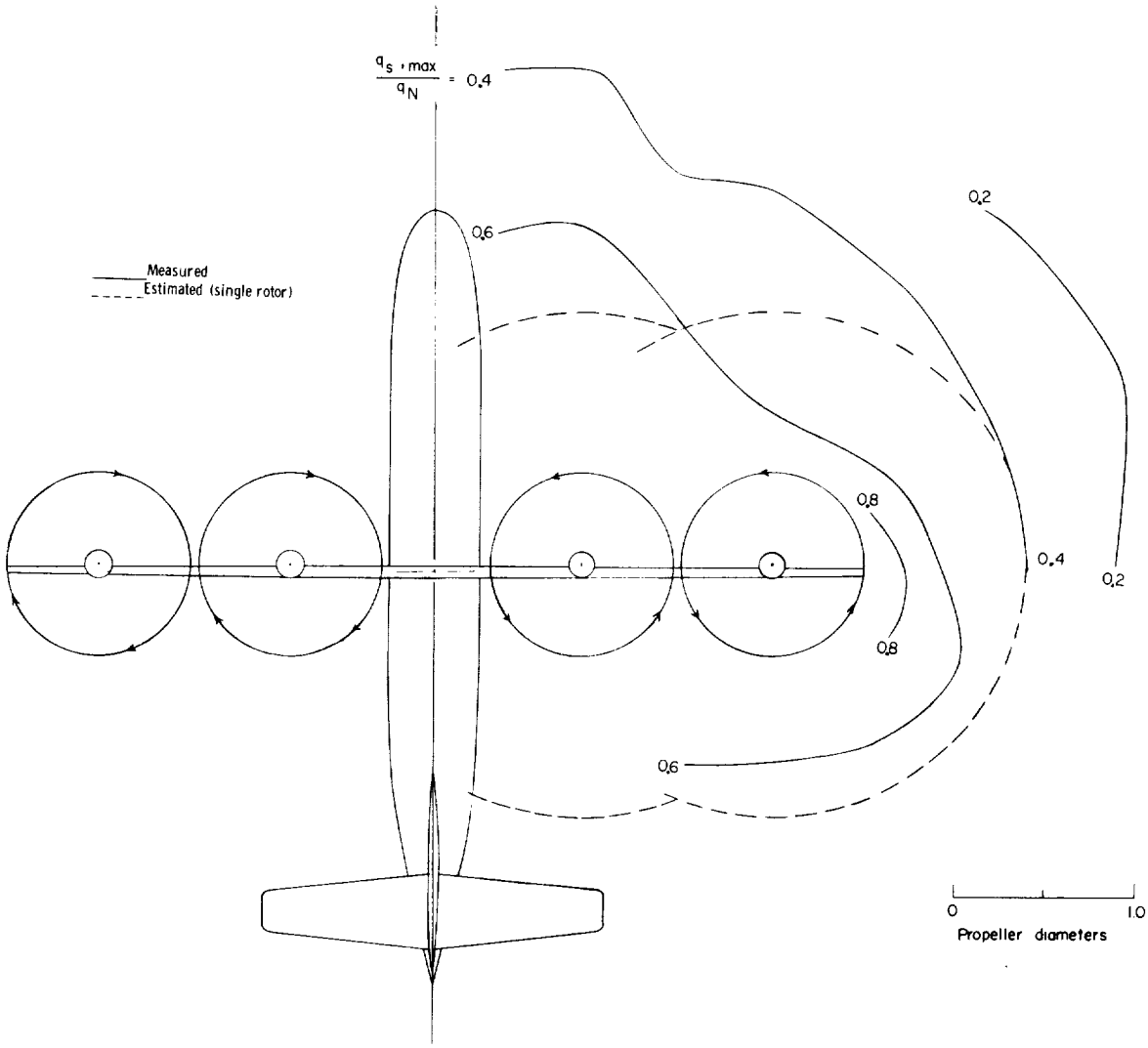

(a) Four-propeller model.

Figure 7.- Dynamic-pressure contours of the models tested. Data taken from figures 4, 5, and 6.

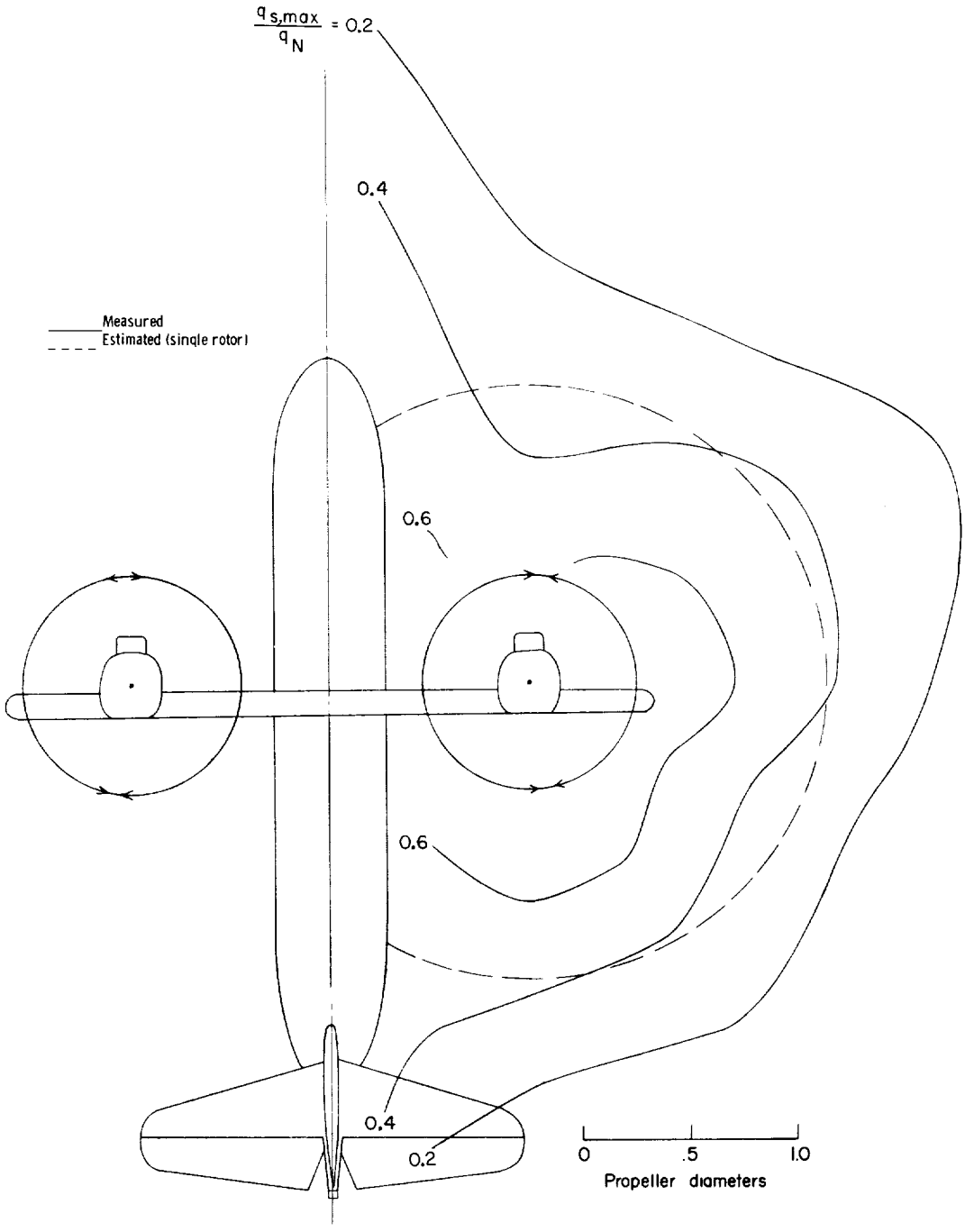

(b) Hiller X-18 model.

Figure 7.- Continued.

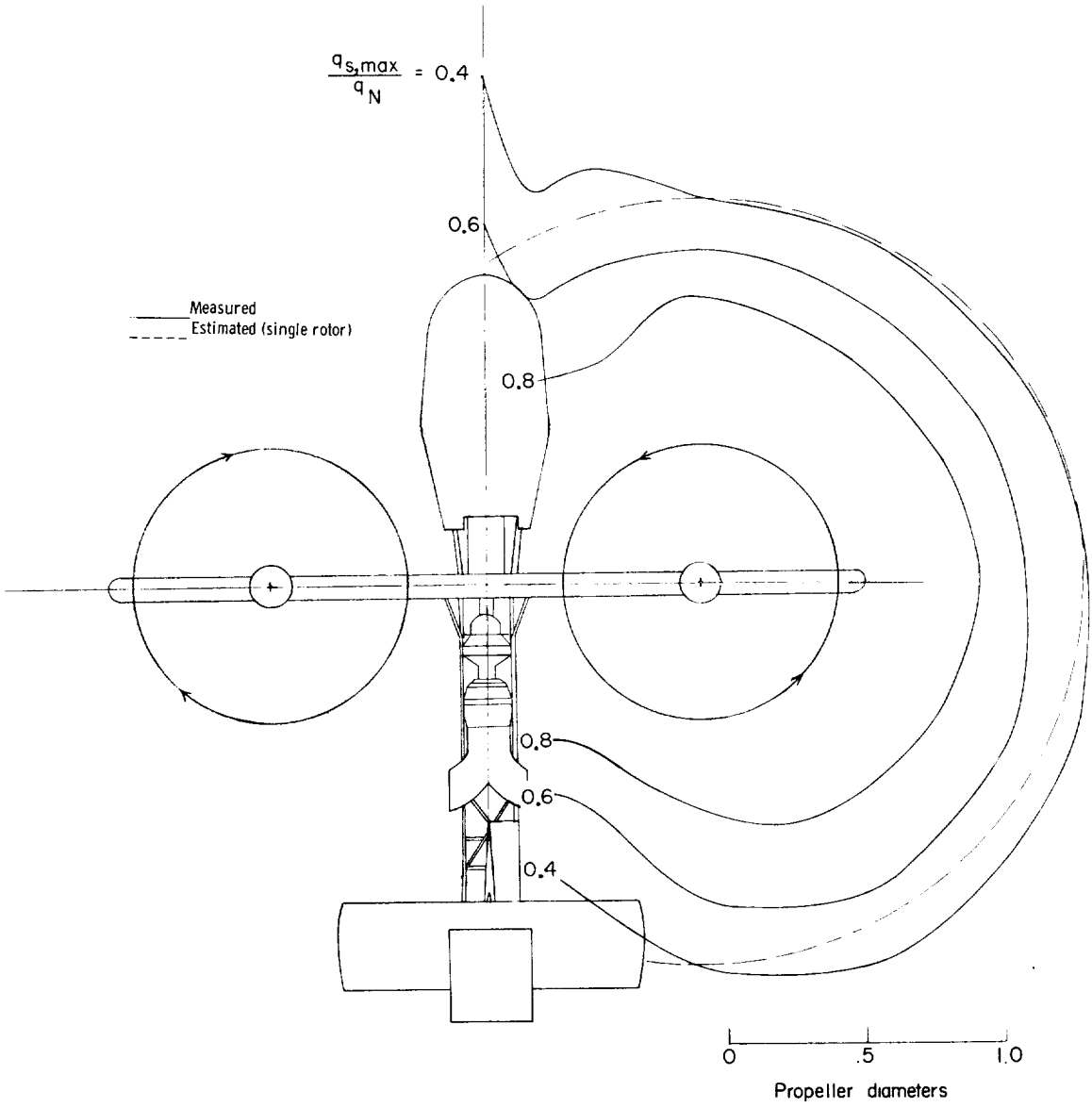

(c) VZ-2 model.

Figure 7.- Concluded.

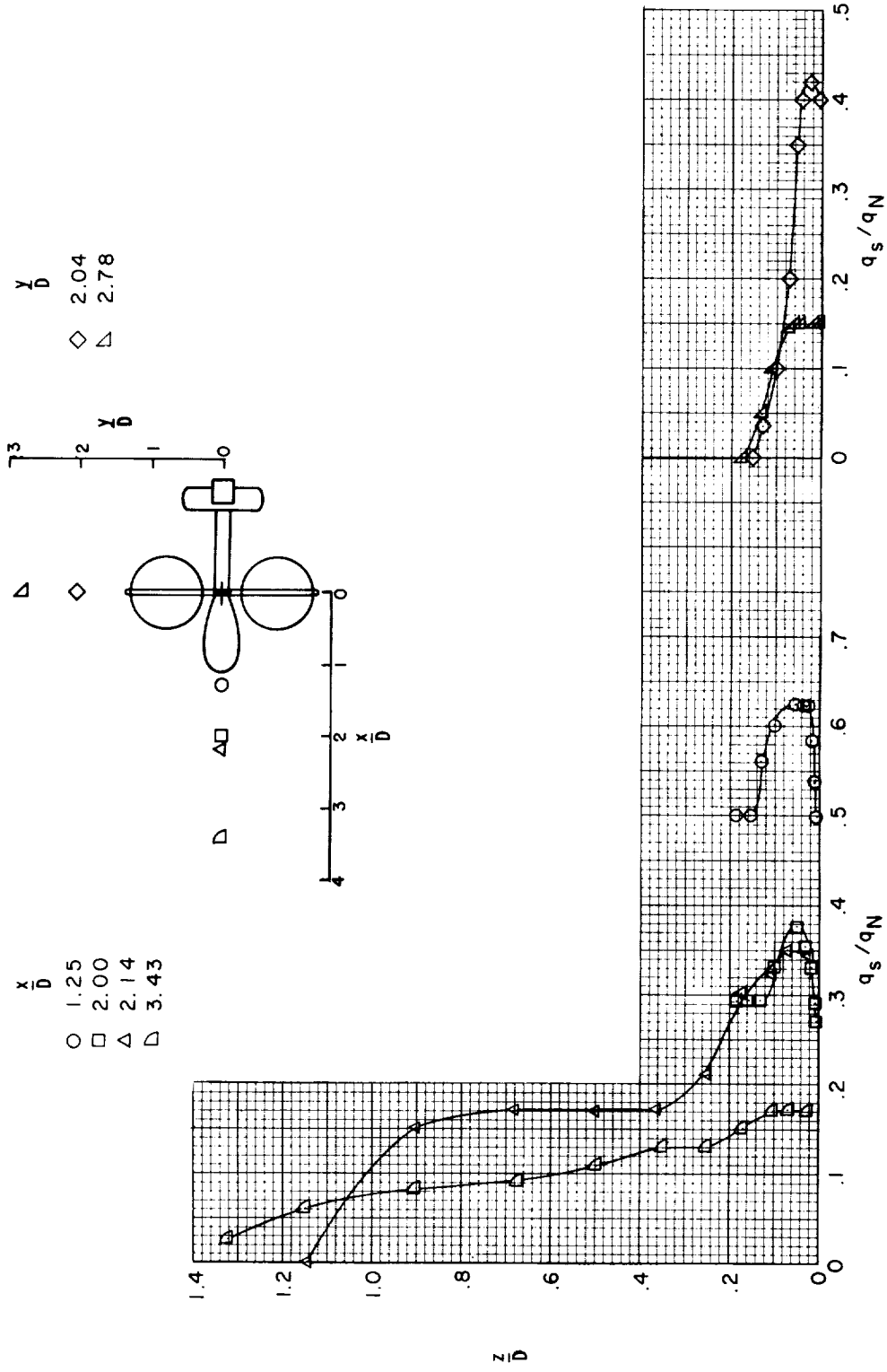

Figure 8.- Comparison of dynamic-pressure profiles near the ground at stations along the plane of symmetry and at stations in the extended plane of the wing of the VZ-2 model.

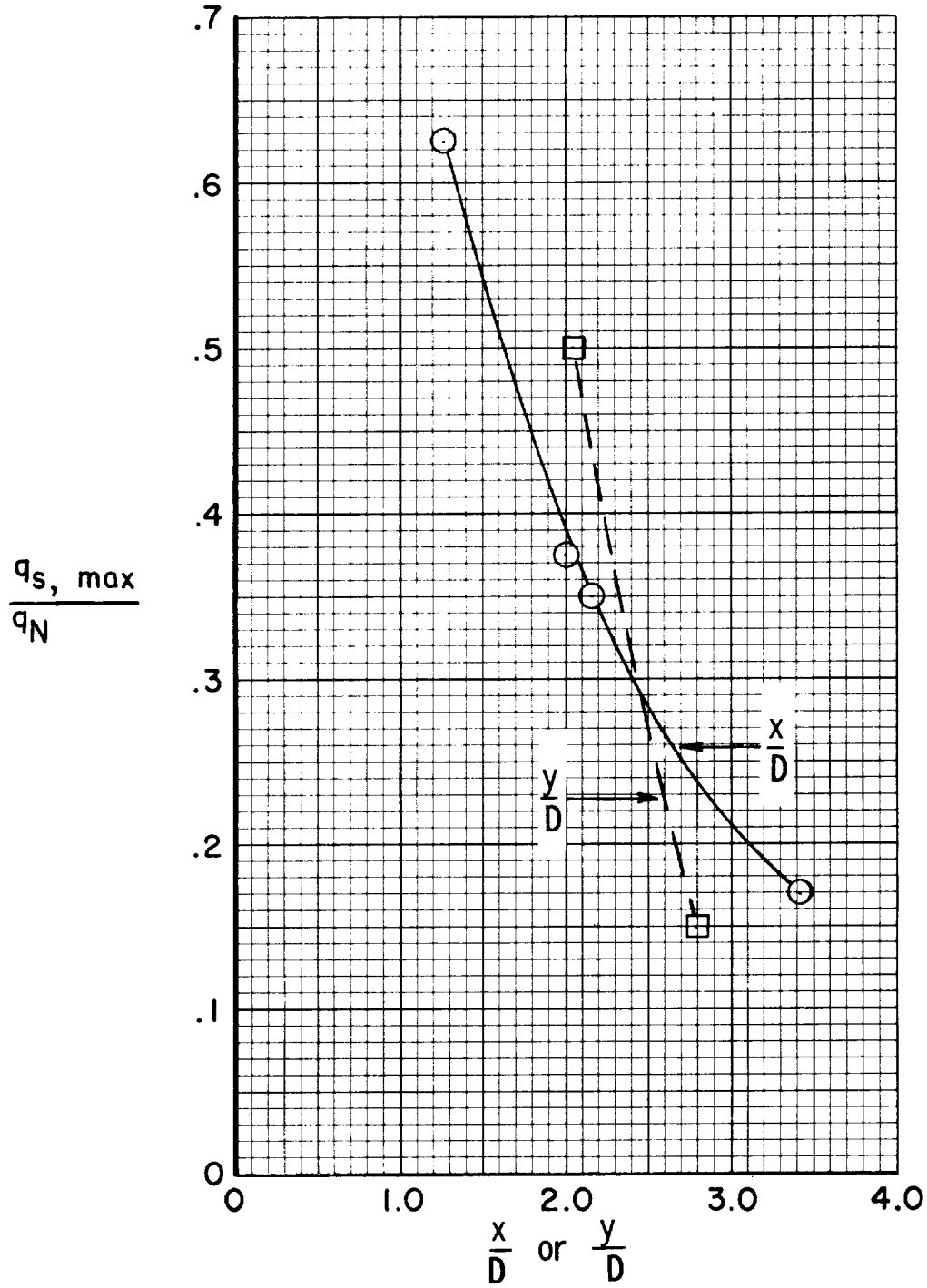

Figure 9.- Variation of maximum dynamic pressure at stations outward from the center of the VZ-2 model (data from fig. 8).

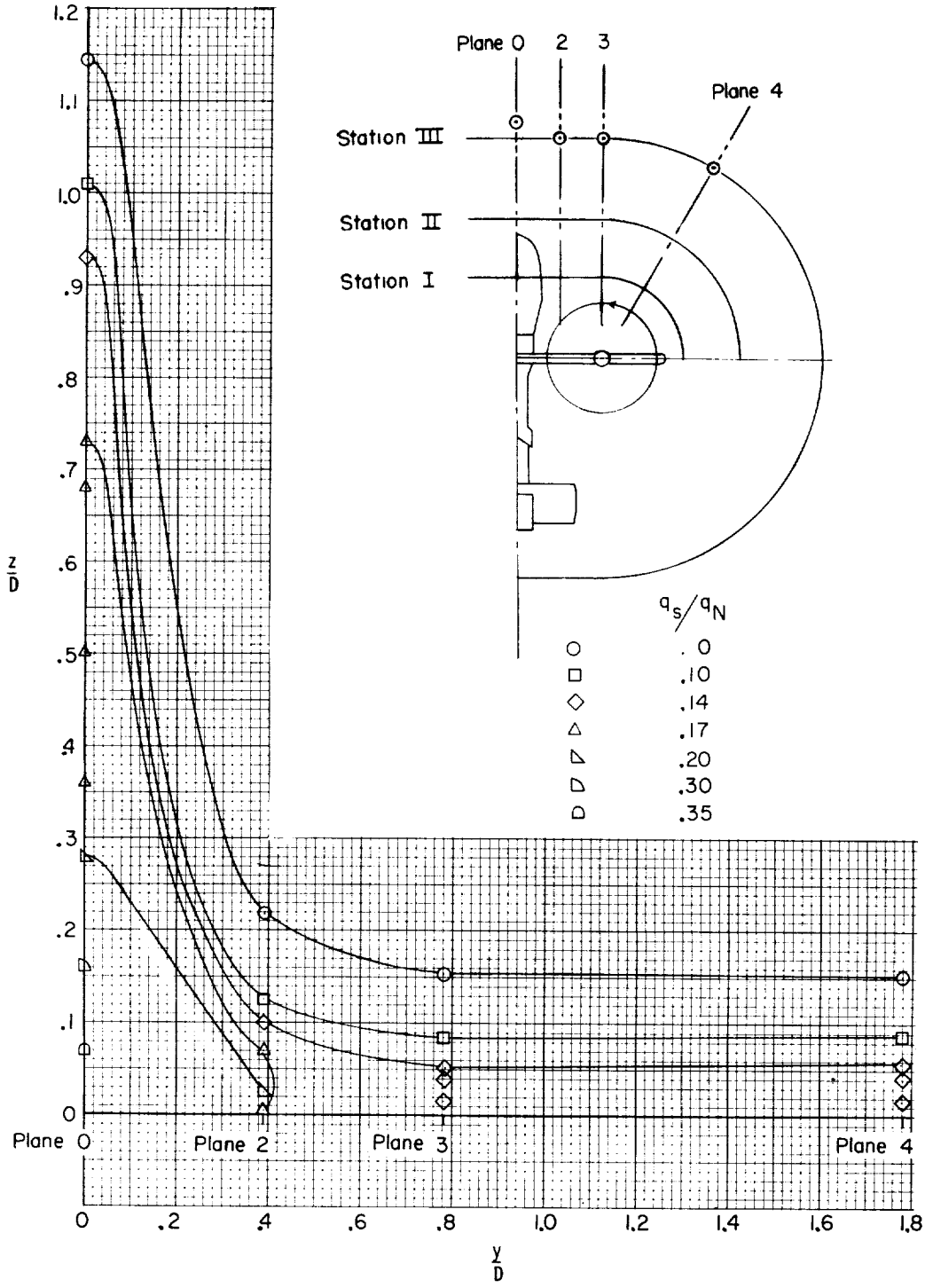

Figure 10.- Dynamic-pressure contours for the VZ-2 model cross plotted from figures 6(c), (d), (e), and figure 8.

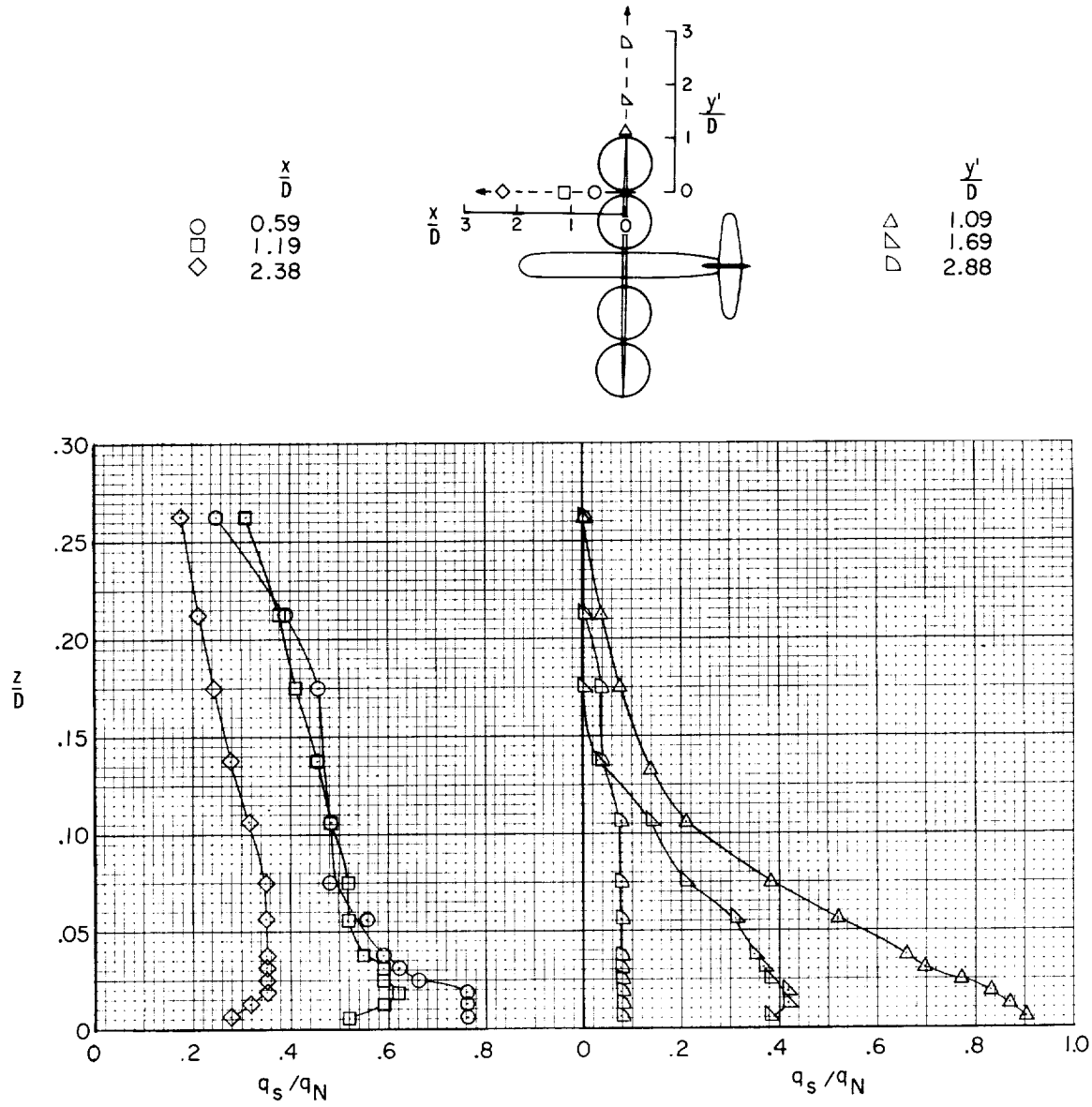

Figure 11.- Comparison of dynamic-pressure profiles near the ground at stations in the extended plane of the wing and at stations fore and aft of the wing plane of a four-propeller configuration.

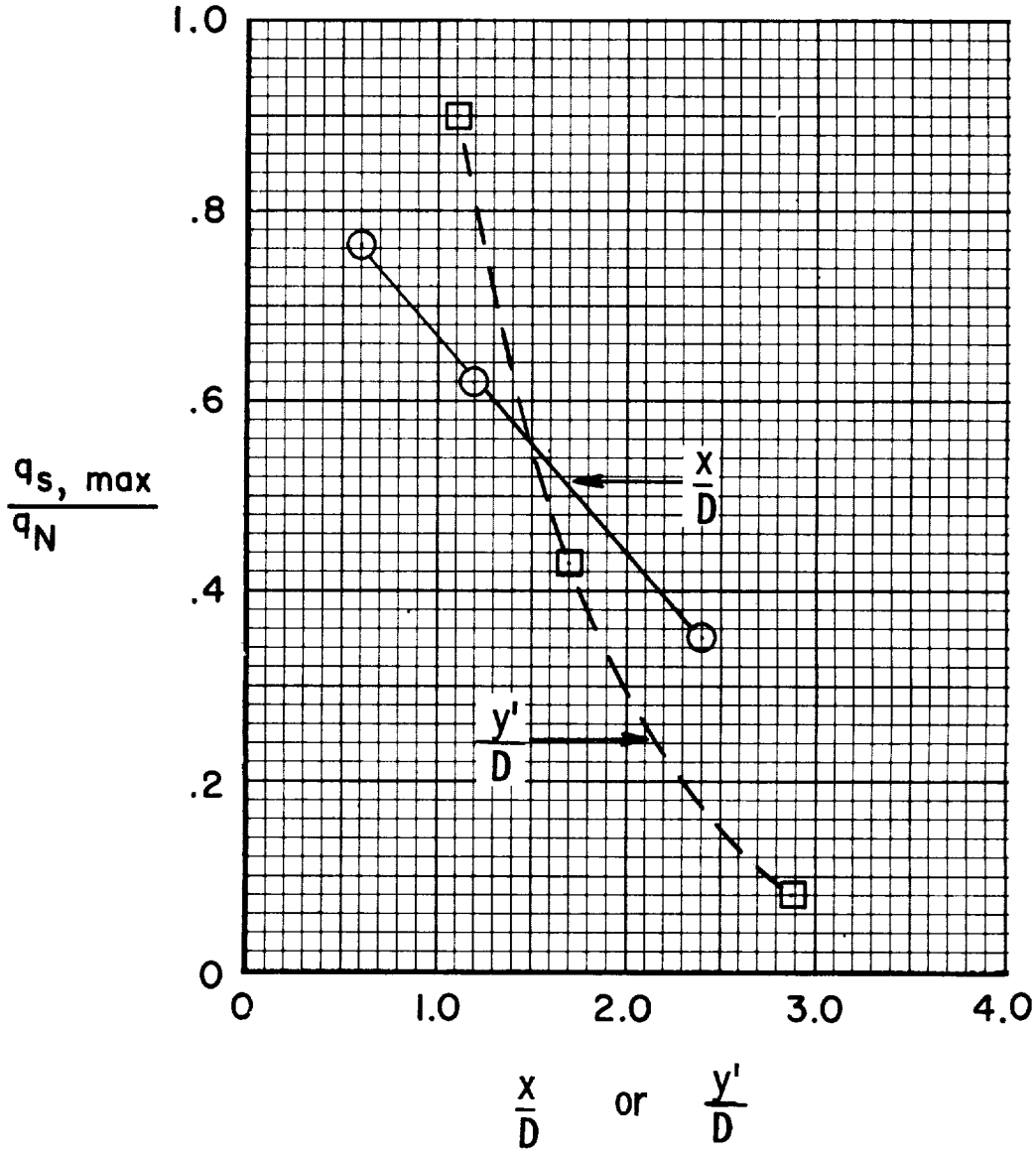

Figure 12.- Variation of maximum dynamic pressure at stations outward from a point between two adjacent propellers of the four-propeller model. (Data from fig. 11.)

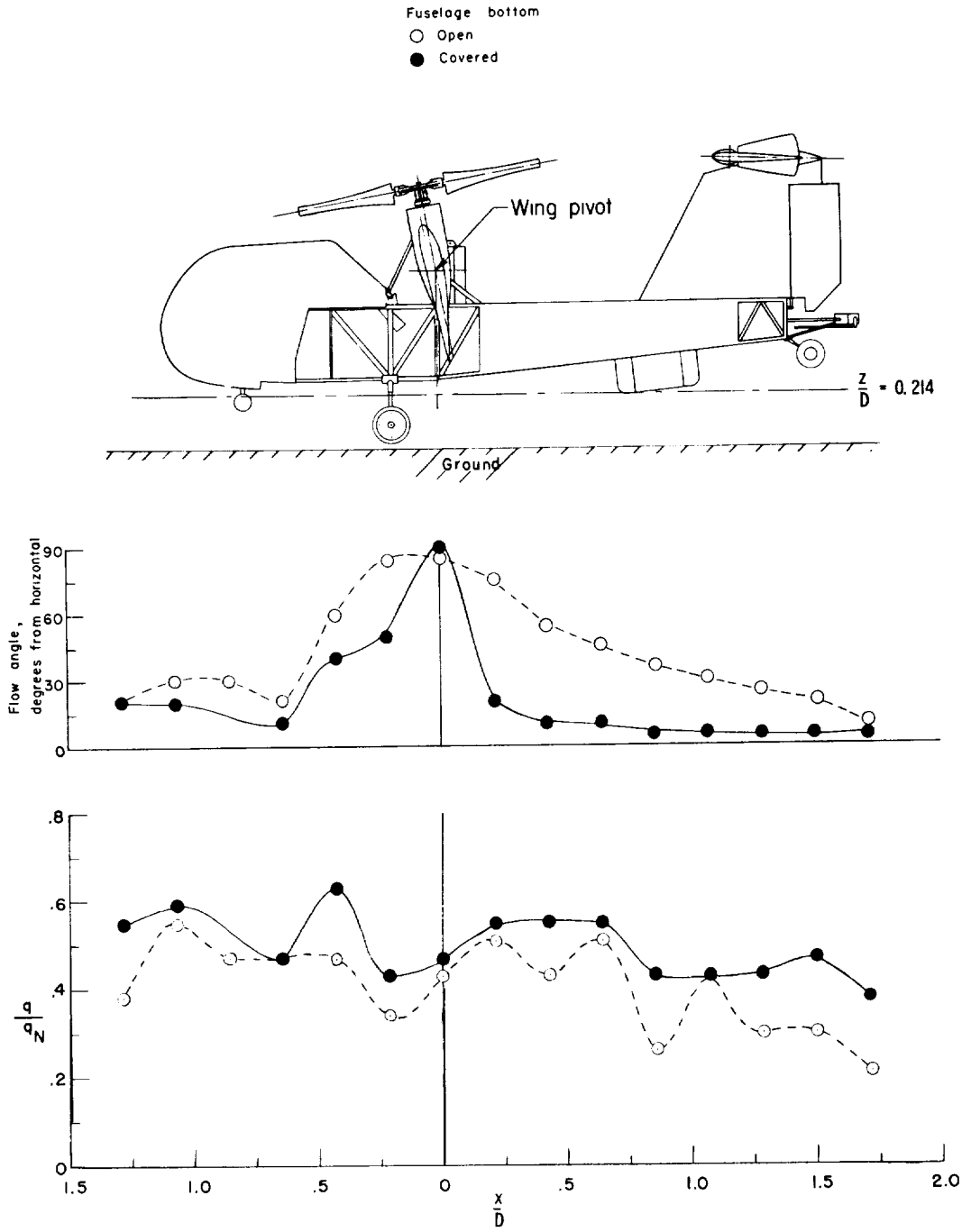

(a) Plane of symmetry.

Figure 13.- Dynamic-pressure ratios and angles of flow near the bottom of the fuselage of the VZ-2 model.

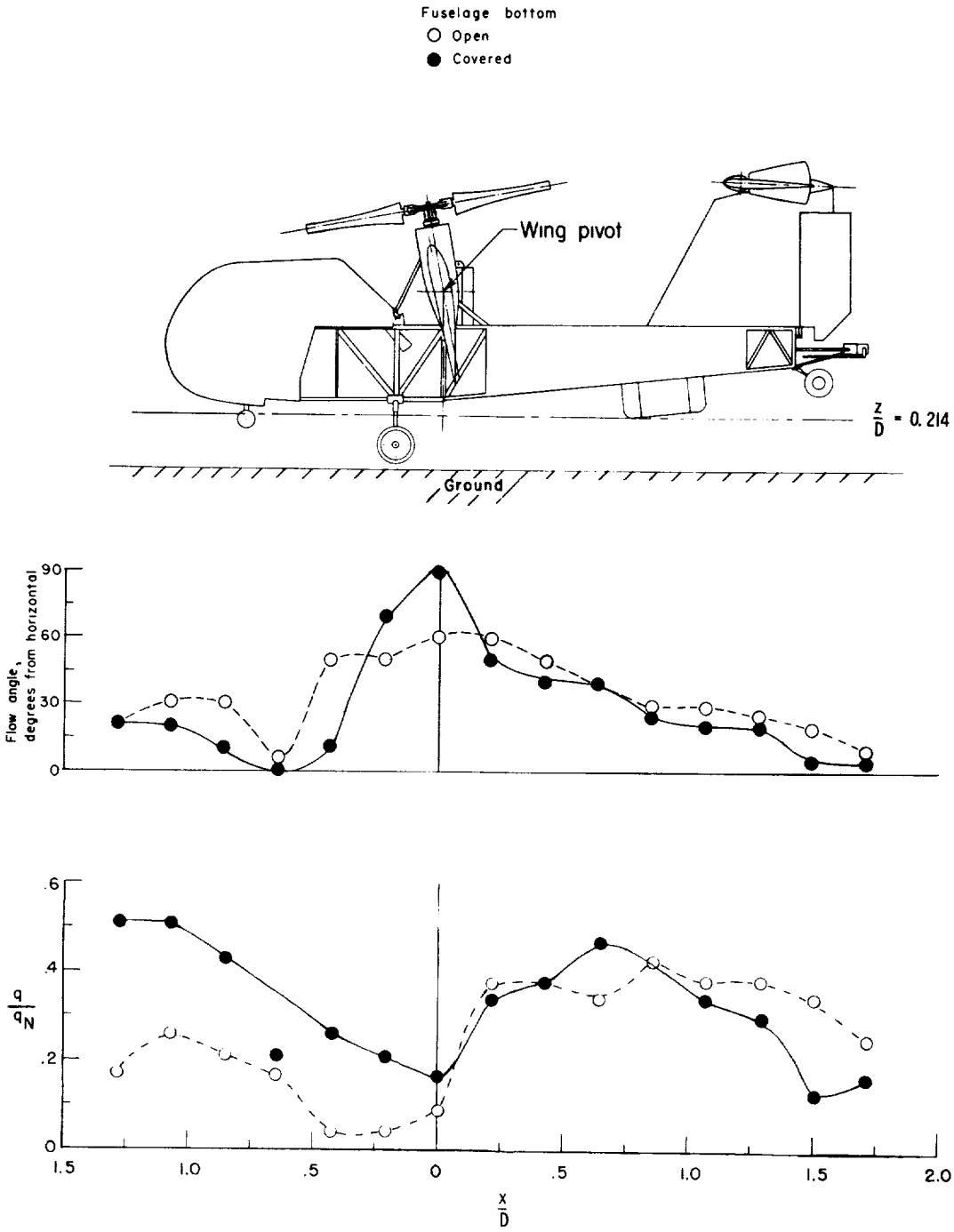

(b) y/D = 0.11.

Figure 13.- Continued.

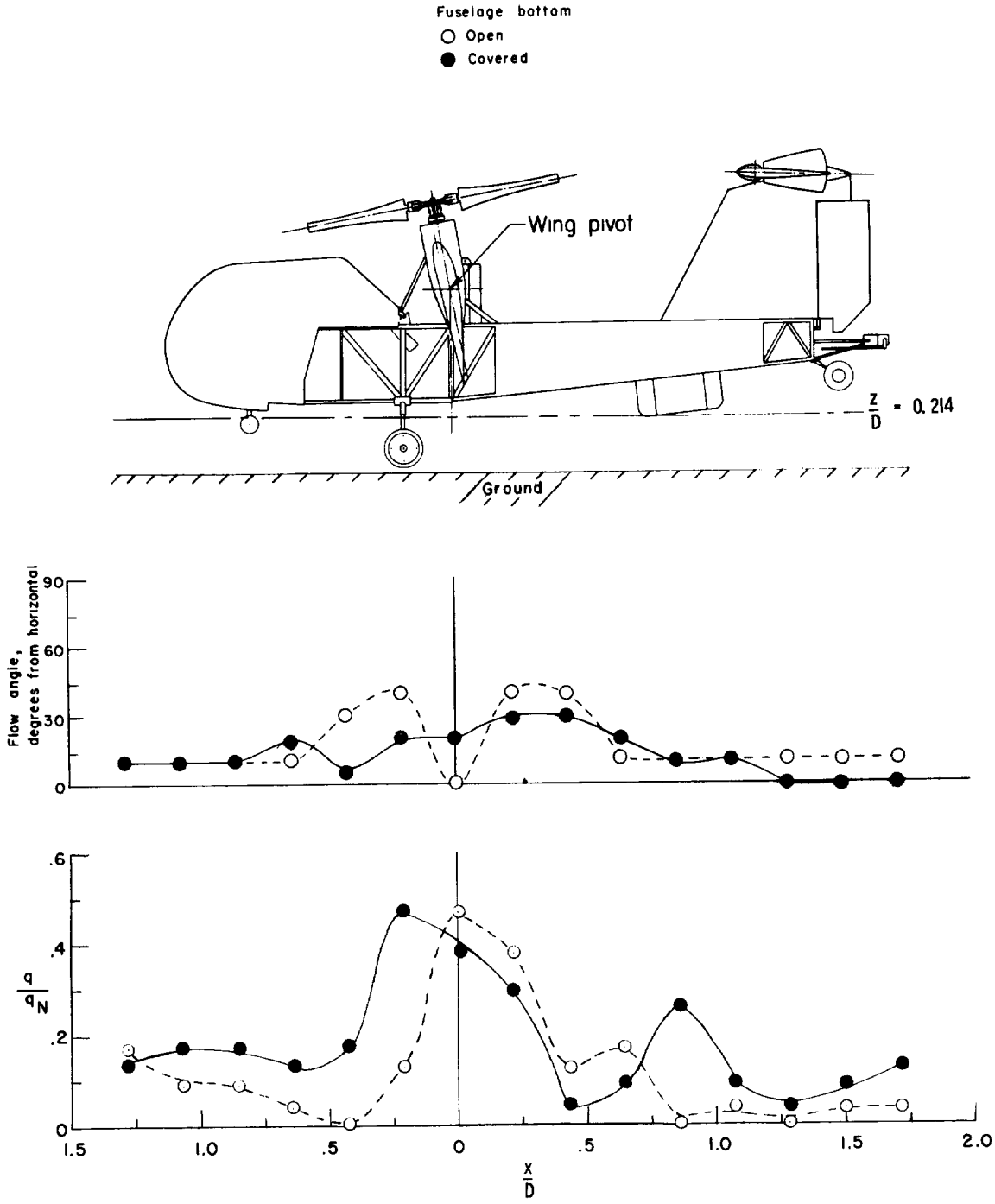

(c) y/D = 0.22.

Figure 13.- Concluded.

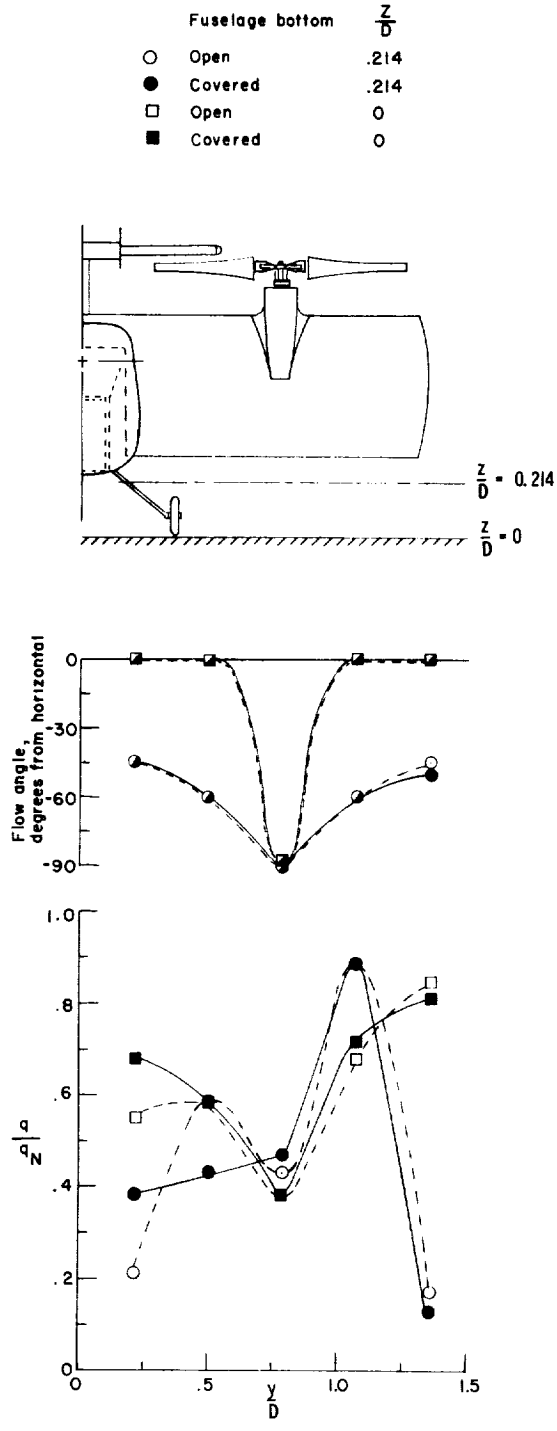

Figure 14.- Dynamic-pressure ratios and angles of flow in the plane of the wing of the VZ-2 model.

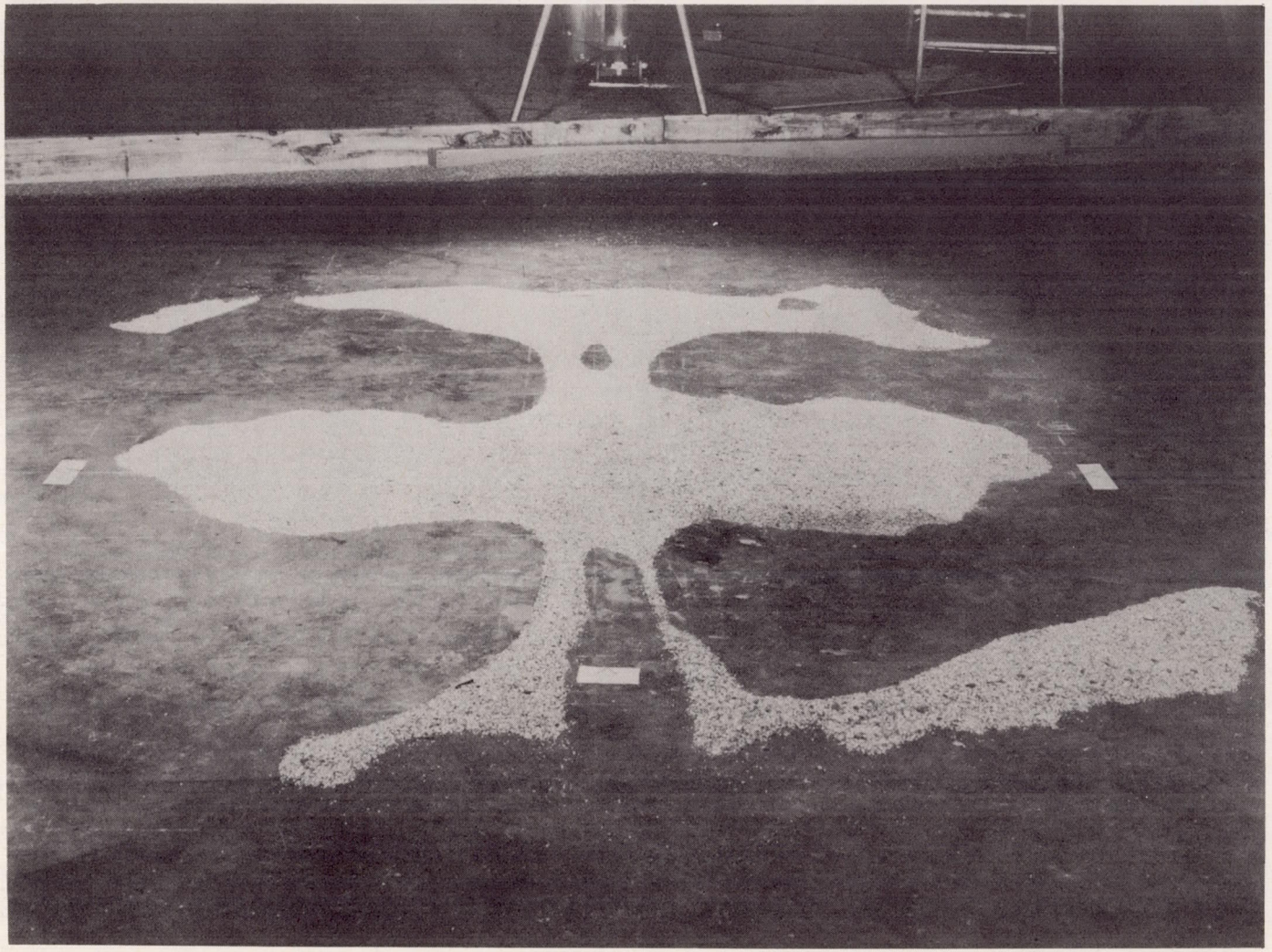

L-61-1110

Figure 15.- Photograph (taken from front of the model) of pattern of small gravel remaining after erosion test of VZ-2 model. Tape strips indicate outer limits of nose, tail, and wing tips.

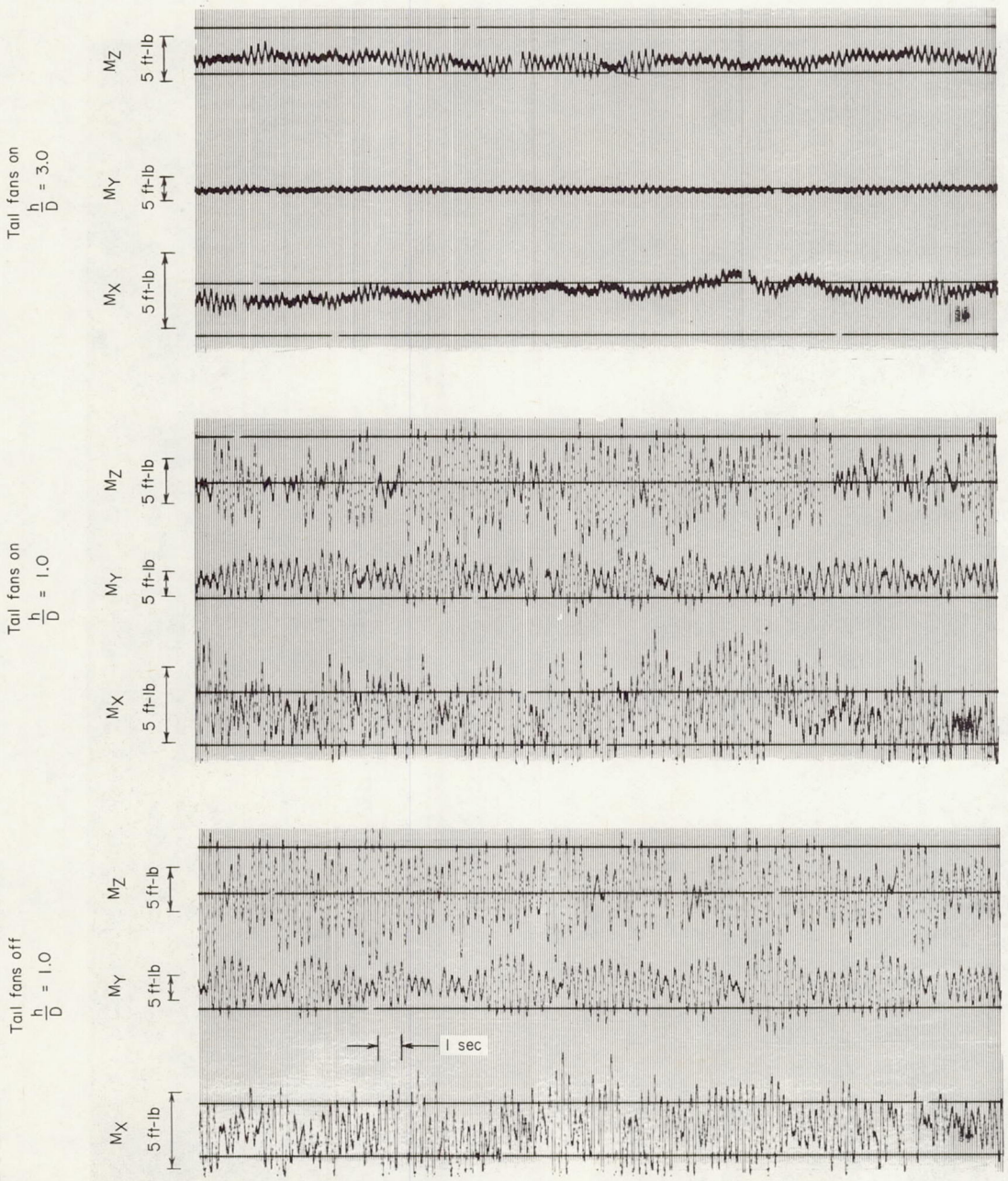

(a) Fuselage bottom open.

Figure 16.- Oscillograph records of the random yawing, rolling, and pitching moments measured during the hovering tests of the VZ-2 model in and out of ground effect. Propeller speed = 2,400 rpm.

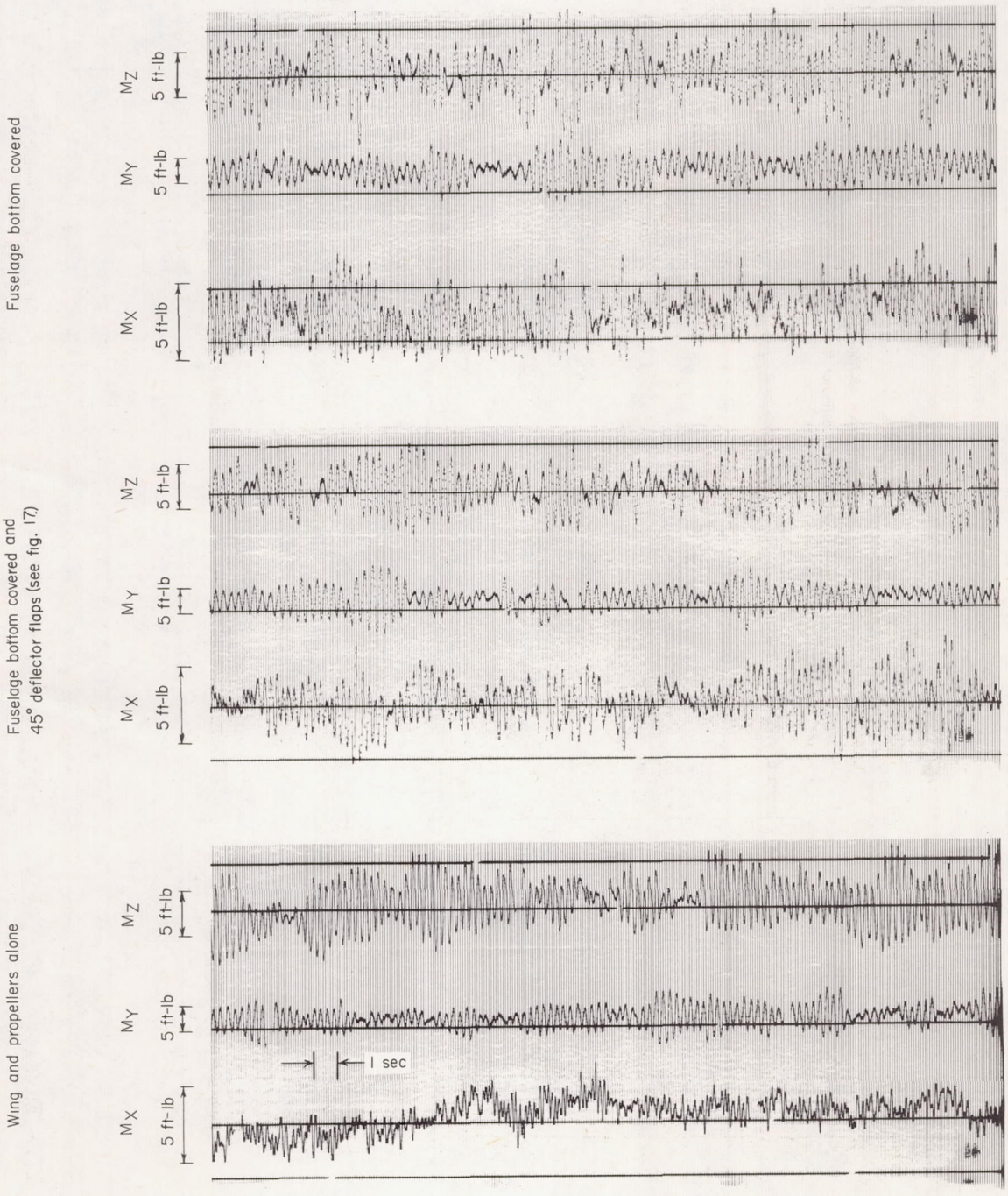

(b) Tail fans off; h/D = 1.0.

Figure 16.- Concluded.

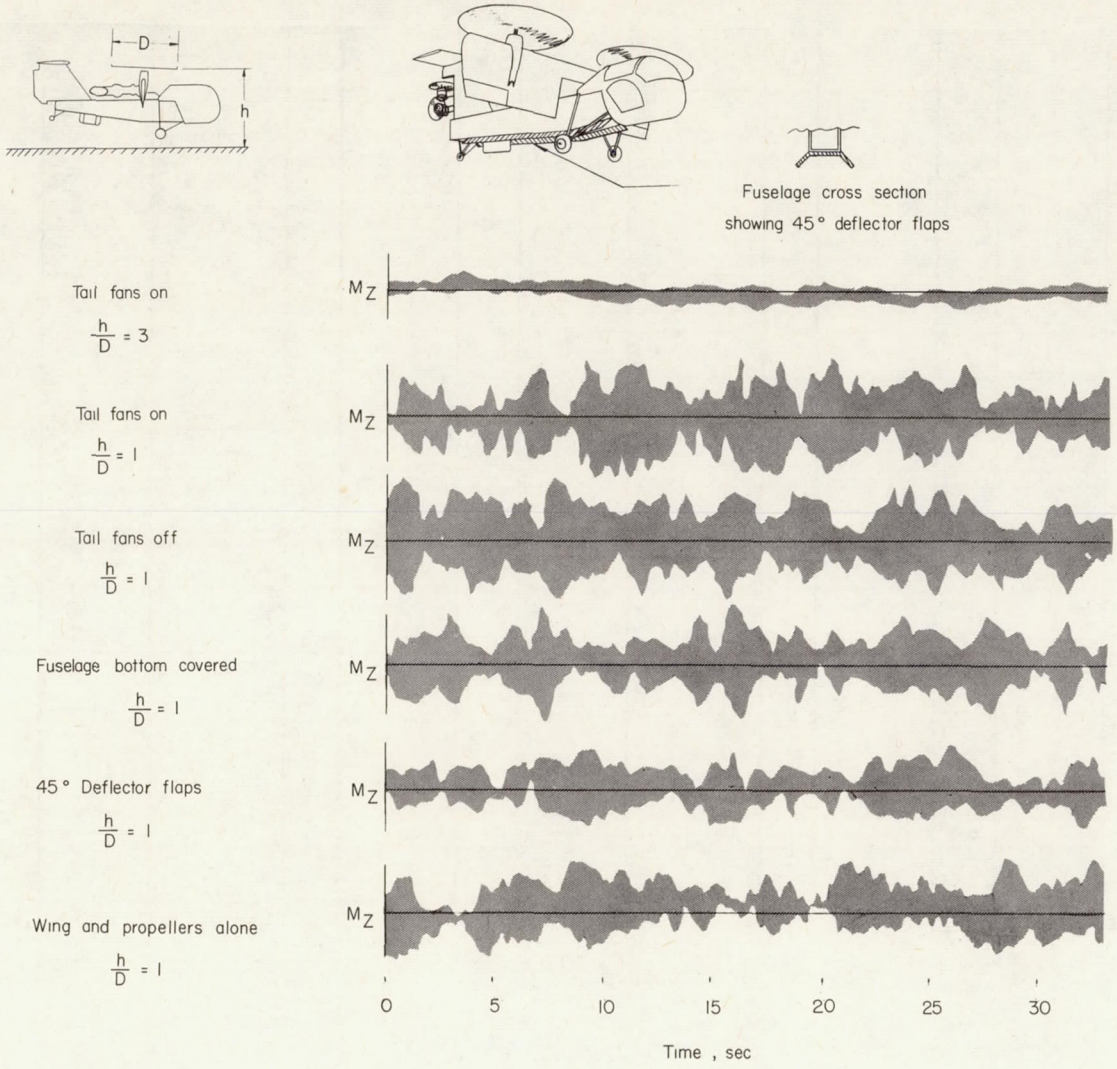

Figure 17.- Envelopes of yawing-moment traces recorded in hovering tests of 1/4-scale model of VZ-2 aircraft in and out of ground effect. Controls fixed.

NASA-Langley, 1962 L-1983